

Organic matter preserved in modern ooids from  
Shark Bay and the Bahamas

by

Aimée L. Gillespie

B.S., Geology  
California Institute of Technology (2009)

Submitted to the Department of Earth, Atmospheric, and Planetary Sciences  
in partial fulfillment of the requirements for the degree of

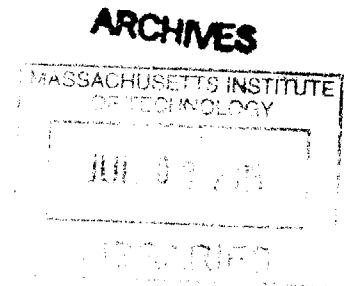
Master of Science in Earth and Planetary Science

at the

Massachusetts Institute of Technology

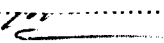
June 2013

© 2013 Massachusetts Institute of Technology.  
All rights reserved.



Signature of Author .....  
 Department of Earth, Atmospheric, and Planetary Sciences  
May 21, 2013

Certified by .....  
 Roger Summons  
Professor of Geobiology  
Thesis Supervisor

Accepted by .....  
 Robert van der Hilst  
Schlumberger Professor of Earth and Planetary Sciences  
Head of Department



# Organic matter preserved in modern ooids from Shark Bay and the Bahamas

by

Aimée L. Gillespie

Submitted to the Department of Earth, Atmospheric, and Planetary Sciences  
on May 21, 2013 in partial fulfillment of the requirements for the degree of  
Master of Science in Earth and Planetary Science at the  
Massachusetts Institute of Technology

## Abstract

Ooids — small, concentrically laminated carbonate grains — are an important component of the sedimentary rock record, yet many details of their formation are not well understood. In particular, the role of microorganisms and organic matter is controversial. To learn about the geochemical and biological environment in which ooids form, modern ooids from two localities (Carbla Beach, Shark Bay, Western Australia, and Highborne Cay, Bahamas) were dissolved incrementally. Analysis of radiocarbon by accelerator mass spectrometry of CO<sub>2</sub> liberated during incremental dissolution of ooid carbonate provided information about the timescale of ooid formation and the ages of these particular ooids: Highborne Cay ooids began forming at least 1,000 years ago, with a possible erosional event approximately 500 years ago, and Carbla Beach ooids began forming at least 1,250 years ago. Each dissolution step liberated lipids, which were analyzed by gas chromatography-mass spectrometry and gas chromatography-isotope ratio mass spectrometry. The organic component of the ooids, which is ~3% by weight, is composed primarily of straight-chain, saturated fatty acids with chain lengths that vary between C=12 and C=30. Also present are branched, short-chain fatty acids, and long-chain fatty ketones. Most compounds have  $\delta^{13}\text{C}$  values that fall between -12‰ and -30‰, and  $\delta\text{D}$  values between -50‰ and -150‰. The distribution of lipids and their stable isotope signatures, which is consistent through incremental dissolutions, provides a fingerprint of the complex microbial community that lives in close proximity to growing ooids. These results suggest it is possible that this consortium of microbes alters the microenvironment of growing ooids in such a way that stimulates carbonate precipitation and protects ooids from dissolution.

Thesis Supervisor: Roger E. Summons  
Title: Professor of Geobiology



## Acknowledgements

I am grateful for the support of my adviser, Roger Summons, and everyone in the Summons Lab. For the past three years I have been supported and encouraged by everyone in the lab, and I am happy to have spent time working with such wonderful scientists and individuals. My lab mentor, Sara Lincoln, has been particularly supportive throughout grad school, especially now as we both work to finish our theses. My thanks extend beyond the lab to the other faculty, students, visitors, and staff who work (or have worked) in E25 and the Green Building, which has become my corner of campus. There are too many of you to list, a fact that makes me smile.

I have been privileged with generous support throughout my tenure at MIT as a National Science Foundation Graduate Research Fellow, and as an MIT Presidential Fellow.

I have enjoyed many valuable discussions with collaborators on my thesis project. I appreciate feedback and insight regarding this project and this document from David McGee and Sara Pruss, my thesis committee members. Mark Roberts and Steven Beaupre from NOSAMS, WHOI, have been invaluable in developing the methods for measuring radiocarbon in my samples. The scientists who participated in the Shark Bay sample collecting field trip in June 2011, including Ginny Edgcomb, Joan Bernhard, Peter Visscher, Malcolm Walter, Bill Schopf, and many, many others, demonstrated to me the depth and breadth of geobiology and geochemistry, and made my time in the outback memorable. Alex Sessions, my former research adviser, continues to support me on this project and in general; his lab ran my samples for hydrogen isotope analysis. Florence Schubotz helped me run my samples on the LC-MS for IPLs and GDGTs. There are many other people involved in this and related projects, and I am lucky to work with them.

I enjoyed the opportunity to mentor two students briefly in the lab on projects related to ooids and stromatolites, and I'd like to recognize them for their patience and enthusiasm. Rawan Edan and Kiara Gomez, you are both awesome.

MIT has afforded me the opportunity to take classes with amazing faculty outside my department. I'd like to thank Elizabeth Cavicchi and Seth Mnookin for helping me become a better science educator and communicator. Another thank you to Michael Dixon and the lovely people at Parkside Christian Academy, where I spent IAP '13 as an "extern."

Those closest to me, my family and friends, deserve the most recognition, for they are the ones that have seen me through the ups and downs of the past three years. You know who you are, and you are wonderful.



# Table of Contents

<b>Abstract</b> .....	<b>3</b>
<b>Acknowledgements</b> .....	<b>5</b>
<b>Introduction</b> .....	<b>9</b>
Background and Geologic Importance .....	9
Ooid Formation and Organic Matter .....	9
Modern Biogeochemical Approaches .....	11
Motivation .....	11
<b>Methods</b> .....	<b>12</b>
Sampling .....	12
Sieving .....	12
Dissolution and Extraction .....	12
A note .....	13
Elemental Sulfur .....	14
Radiocarbon Dating of Organic Matter .....	14
Highborne Cay .....	14
Carbla.....	14
Radiocarbon Dating of Ooid Carbonate.....	15
Gas Chromatography-Mass Spectrometry (GC-MS) Analysis .....	15
Stable Isotope Ratio Mass Spectrometry (IRMS) Analysis.....	15
Intact Polar Lipids (IPL) Analysis .....	16
Glycerol Dialkyl Glycerol Tetraethers (GDGTs) Analysis .....	16
<b>Results</b> .....	<b>17</b>
Sieving .....	17
Extraction .....	19
Elemental Sulfur .....	20
Highborne Cay .....	20
Carbla.....	20
Radiocarbon Dating of Organic Matter .....	21
Highborne Cay .....	21
Carbla.....	22
Radiocarbon Dating of Ooid Carbonate.....	23
Highborne Cay .....	23
Carbla.....	24
Lipid distribution .....	25
Stable Carbon Isotopes .....	36
Straight Chain Saturated FAMES .....	36
Branched FAMES .....	36
Long Chain Ketones.....	36

Stable Hydrogen Isotopes .....	40
Lipids .....	40
Water .....	40
Intact Polar Lipids (IPL) and Glycerol Dialkyl Glycerol Tetraethers (GDGTs) .....	40
<b>Discussion .....</b>	<b>44</b>
Elemental sulfur .....	44
Radiocarbon Dating of Organic Matter .....	44
Highborne Cay .....	44
Carbla .....	44
Radiocarbon Dating of Ooid Carbonate .....	45
Highborne Cay .....	45
Carbla .....	45
Lipid distribution .....	45
Stable Carbon Isotopes .....	46
Hydrogen Isotopes .....	47
Lipids .....	47
Intact Polar Lipids (IPL) and Glycerol Dialkyl Glycerol Tetraethers (GDGTs) .....	47
<b>Conclusions .....</b>	<b>48</b>
Future Work .....	48
<b>Works Cited .....</b>	<b>49</b>



# Introduction

## ***Background and Geologic Importance***

Ooids are small, spheroidal calcium carbonate grains. A cross section of the ooid reveals its internal structure: a nucleus, which can be a small shell fragment or other detrital material, and a cortex of alternating layers of calcium carbonate and organic material. There may be other features, including boreholes that crosscut the internal fabric.

Ooids are ubiquitous throughout the sedimentary geologic record: as oolites they occur in the oldest well-preserved sedimentary rocks (the 3.49 Ga Dresser Formation (Noffke et al., 2011)), and continue throughout the rock record all the way to modern beaches. Ooids comprise the beach sand of a handful of modern marine environments including Shark Bay, Western Australia, and the Bahamas, as well as some lacustrine localities like the Great Salt Lake (Sandberg, 1975) and Lake Geneva (Plee et al., 2008).

Despite their apparent prevalence throughout Earth history, the controls on the formation of ooids, in modern environments and in the distant past, are not well constrained. Some factors that are believed to govern ooid precipitation include water temperature, water depth and energy, and aquatic chemistry, including the pH and concentration of calcium ions and carbonate ions (Simone, 1981).

The occurrence of ooids with stromatolites is also of particular importance. Stromatolites are laminated sedimentary structures, widely interpreted as lithofied microbialites, although their biogenicity is still a topic of debate. Fossil stromatolites found in Archean rocks are regarded as the first macroscopic fossils (Allwood et al., 2006). The association of stromatolites and oolites dates back to the Archean. One of the oldest occurrences of the association is known from the 2.72 Ga Tumbiana Formation, Fortescue Group, Pilbara Block in Western Australia (Paul et al., 2011).

Modern stromatolites such as those in the Bahamas and in Shark Bay, Western Australia are associated with ooids. In some cases, such as in modern Bahamian stromatolites and microbiloites, ooids become trapped in the microbial mat and bound in the stromatolite, forming large fraction of the lithographic component of the stromatolite (Decho et al., 2005; Dupraz and Visscher, 2005).

## ***Ooid Formation and Organic Matter***

Ooid formation has been studied in a laboratory setting, which has helped to constrain the conditions suitable for ooid formation (Davies et al., 1978). However, ooid formation in situ is not completely understood. In particular, the role of microorganisms in ooid formation has been highly contested. Some people believe that ooid formation is a completely abiotic process, one which is dependent exclusively on physical and

chemical factors (Duguid et al., 2010). Others believe that microorganisms are actively involved in the mineral precipitation and ooid formation (Brehm et al., 2006; Davies et al., 1978). In between these two extremes are other possibilities, such as that the presence of organic material facilitates ooid formation, or that microorganisms may alter the geochemistry of the local environment in such a way that makes carbonate precipitation and ooid formation favorable (Reitner et al., 1997).

It has been known that ooids contain a significant amount of organic material since the 1960s (Mitterer, 1968, 1972), and in the literature said organic matter is referred to in general terms like "humic acids, etc," but detailed analyses of the composition of the organic matter using modern analytical techniques is only recently being explored (Edgcomb et al., 2013; Reitner et al., 1997). A geochemical analysis of the composition and distribution of lipids is a useful way to gain insight into the diversity of microbial flora represented in a given environment, especially in old samples. Unlike many other biomolecules (nucleic acids, proteins, carbohydrates) that provide taxonomically specific information but are easily degraded, lipids can persist in the environment for billions of years. Fatty acids are one such class of molecules: through their chain lengths, patterns of unsaturation, and branching, they encode information about their parent organisms. Other such molecules are alkanes, fatty alcohols and ketones, and terpenoids such as steroids and hopanoids.

Experiments performed in the 1960s and 1970s by Chave and Suess found a relationship between carbonate precipitation and organic matter (Chave, 1965; Chave and Suess, 1970). Chave (1965) showed that natural carbonate particles in seawater did not react with the water when it was acidified with dilute HCl, although clean calcite did react. Attempts to get particles to react with seawater, by heating cold waters or cooling warm waters failed to cause precipitation or dissolution. Chave remarked on the anomalous stability of aragonite and a range of magnesium calcites in seawater, and upon the supersaturation of near-shore Bermudan waters for all but the most soluble phases in summer, and undersaturation in winter. They also showed that marine carbonate particles failed to react with seawater *unless* they were first treated with peroxide, when reaction took place (Chave and Suess, 1967). More experiments that found that CaCO<sub>3</sub> does not precipitate until after some of the dissolved organic compounds have been precipitated.

These experiments are believed to indicate that CaCO<sub>3</sub> cannot precipitate from seawater containing the normal amount of dissolved organic compounds. Taken together, these findings suggest the importance of organic material in ooid formation: dissolved organic carbon may protect ooids from dissolution, and at the same time may hinder carbonate growth. Perhaps the precipitation of organic rich layers is a necessary step in ooid formation; the organics protect interior carbonate layers from dissolution, and prepare the grain for the next phase of carbonate precipitation.

Another fundamental question regarding ooid formation is one of timescale. Ooids can form in laboratory conditions in a matter of weeks (Davies et al., 1978), but this is not necessarily a good analog of environmental ooid formation. By radiocarbon dating of

the mineral component of the ooid, we can better constrain how long it takes ooid to form in situ.

### ***Modern Biogeochemical Approaches***

Forthcoming work led by the Summons Lab, and which I participated in, was the first detailed comparative study of organic compounds associated with ooids from different locations and of different ages (Summons et al., Under Review). Modern ooids were collected from three localities in the Bahamian archipelago, and from one locality in Shark Bay, Western Australia. Additionally, Holocene oolites were collected from outcrops at two localities in the Bahamas. Lipid extraction and analysis, as well as stable isotopic ( $^{13}\text{C}$  and  $^2\text{H}$ ) analysis were performed on these samples.

In this study, the authors conclude that lipid distributions extracted from beach ooids and Holocene oolites had many similarities, including biomarkers for a suite of diverse microorganisms including photoautotrophs, heterotrophs, and sulfate-reducing bacteria.

This work is supported by recent research (Edgcomb et al., 2013). In this study of microbial diversity in the oolitic sand of Highborne Cay, the authors find a similar consortium of microorganisms. The use of molecular indicators allows them greater taxonomic specificity when identifying the organisms. Additionally, they found “significant overlap in the taxonomic groups” when comparing the microbial diversity of ooids and stromatolites and other microbialites from the same area. This finding strengthens this relationship between ooids and stromatolites, in particular the microbial community that is largely responsible for microbialite formation.

Their findings lead them to hypothesize that a biofilm of colonizing microorganisms surrounds the ooids and contribute to ooid cortex growth. Lipids from this suite of organisms are incorporated in the carbonate matrix throughout ooid formation and growth, and provide insight into the local environment at the time of formation.

### ***Motivation***

This recent work, which I worked on before starting this separate, more in-depth investigation, suggests that more insight into the process of ooid formation might be gained by analysis of lipids liberated during a sequential dissolution of the ooid carbonate matrix. This thesis provides the first attempt at sequential dissolution of modern ooids with the intention of analyzing the organic material trapped within the ooid cortex. Techniques of organic geochemistry and isotope geochemistry were used to characterize the remnants of the microbial community present throughout the formation of modern ooids. Specifically, we are looking for molecules that are known to be lipid biomarkers for taxonomically specific organisms, and for an overall pattern that might act as a fingerprint of the microbial community.

## **Methods**

### ***Sampling***

Samples were collected from Highborne Cay (-76°49'7", 24°43'32") in the Bahamas by Drs. Sabine Mehay and Roger Summons in March 2010.

Samples were collected from Hamelin Pool at Carbla Beach (-26°9'40", 114°12'42") in Western Australia by the author and Dr. Roger Summons in June 2011.

Both samples were collected at low tide, submerged by approximately one meter of water. The samples were collected and stored in large Nasco Whirl-Pak bags and frozen at -20° C until analysis.

### ***Sieving***

The ooids were sorted using a set of seven geologic sieves. This step served several purposes: to remove skeletal fragments and non-ooid detrital particles, which were larger than the ooid grains, and to sort the ooids into an aliquot with similar surface area. This allowed for dissolution of an equal sized "layer" of carbonate during each step in the dissolution.

### ***Dissolution and Extraction***

An aliquot (Highborne = 100 grams, Carbla = 300 grams) of sieved ooids (Highborne = .105 to .177 mm, Carbla = .177 to .250 mm) was extracted with DCM by sonication five times. The ooids were covered with an excess of DCM and placed in a sonicating water bath for 10 minutes. The supernatant was decanted into a clean beaker, and the process was repeated four times. The extract was concentrated under a stream of nitrogen and transferred to a clean vial with a small volume of DCM. This extract of the loosely associated biofilm of lipids was referred to as "d0."

The same ooids were then placed in a 2 L beaker. Approximately 300 mL of "geoclean" water was added to the beaker. Ooids were suspended in the water (Highborne ooids by agitation with a magnetic stir bar, Carbla ooids by vigorous stirring with a glass rod). Enough 12 N HCl (geoclean) was added, dropwise, to dissolve a small fraction (Highborne = 5%, Carbla = 10%) of the calcium carbonate. The resulting water was decanted and saved. The remaining ooids were extracted with DCM by sonication for 10 minutes, three times. They were then washed an additional two to three times by solvent washing with DCM. The combined supernatant (a combination of water and DCM) was placed in a separatory funnel. The organic phase was collected, and the aqueous phase was washed with DCM three to five times. If an emulsion occurred and separation was difficult, more geoclean water was added to the aqueous phase. The

organic extract was combined and concentrated under a stream of nitrogen at 37° C. Once dry, the extract was transferred to a vial with a small volume of DCM. This sample is referred to as “d1,” referring to the extract of the first dissolution of calcium carbonate. The process was repeated to yield extracts d2 through d20 (Highborne) or d10 (Carbla).

To removed the residual inorganic material, each extract was run over a short (~1 cm) column of silica with a modified method (Liu et al., 2011): In brief, a glass column was packed with 1.5 g silica gel and preconditioned with EtOAc; the first fraction (F1), containing apolar neutral lipids and core GDGTs, was eluted with 8 ml EtOAc and the second (F2), containing IP GDGTs with 10 mL MeOH. Both fractions were evaporated to dryness under N<sub>2</sub> before analysis. The fraction of core lipids (F1) was worked up for further analysis, and the fraction of polar lipids has been saved for archival purposes.

The weight of each extract was measured by weighing a 2 mL vial, transferring the sample to the vial with a small volume of DCM, allowing the DCM to evaporate, and weighing the vial again. The difference of the weights is the weight of the sample.

### ***A note***

Because of the small quantity of organic material in the Highborne Cay extracts, the treatment of these samples is different from the Carbla ooids. A small aliquot (10%) of extracts d0 through d10 was derivitized as described below and screened for the presence of organic compounds. The majority of the extracts (90% of samples d0 through d10 and 100% of d11 through d20) were combined with adjacent samples and then sent to NOSAMS for radiocarbon analysis. The rest of the methods described below applies to the small fraction of Highborne Cay samples d0 through d10, and to the Carbla ooid samples, of which there was more starting material (100 grams for Highborne compared to 300 grams for Carbla) and few dissolutions (20 for Highborne Cay versus 10 for Carbla), which led to a richer organic extract.

There are also a few instances when a sample was compromised during workup. In those instances, the result is omitted and replaced with “na” where appropriate.

### ***Derivitization***

The ooid samples were derivitized by methanolysis. Acidic hydrogens are replaced with methyl groups e.g. fatty acids to fatty acid methyl esters (FAMES), which are suitable for GC analysis. The method is as follows:

A solution of anhydrous hydrochloric acid in methanol was prepared by adding 1 mL of acetyl chloride dropwise to 20 mL of cold, anhydrous methanol. The samples were covered in the methanolic HCl solution (~200 to 500 µL) and tightly capped. The samples were then heated (60 to 70° C) overnight, and then allowed to cool to room temperature.

### ***Five Fraction Column Chromatography***

The derivitized samples were separated by liquid chromatography into five fractions based on polarity. Approximately 10 cm of silica gel was packed into a Pasteur pipette. A sequence of five increasingly polar solvents was used to elute the fractions as follows: Aliphatic hydrocarbons were eluted in the first fraction with hexane (1 $\frac{3}{8}$  column dead volume determined empirically for each silica bed) followed by aromatic hydrocarbons in two column dead volumes of 4:1 hexane:DCM, ketones and FAME in two column dead volumes DCM, alcohols in two column dead volumes of 1:1 DCM:ethyl acetate and diols two column volumes of ethyl acetate.

### ***Elemental Sulfur***

Elemental sulfur, which is readily extracted along with the organic material, was removed from the lipid extracts by reaction with copper shot. The surface of the copper shot was activated with hydrochloric acid. The activated copper was added to the solvent extracts. The blackening of the copper into copper sulfides assessed presence of sulfur in each sample. Fresh copper was added until the blackening ceased.

### ***Radiocarbon Dating of Organic Matter***

The radiocarbon of the total lipid extracts recovered from the Highborne Cay and Carbla dissolution experiment were analyzed to determine the age of the organic matter associated with ooids.

#### ***Highborne Cay***

Adjacent samples (d1 and d2; d3 and d4; d5 and d6; d7, d8, and d9; d11 and d12; d13, d14, d15, and d16; d17, d18, and d19) of the Highborne Cay extracts (TLE) were clumped together to meet the minimum mass requirements for the protocol; they were renamed d1' through d7'. There was enough organic material in the freely extractable sample (d0) to analyze separately. Highborne Cay ooids samples d0 and d1' through d7' were sent to the NOSAMS Sample Preparation Lab at WHOI for radiocarbon analysis.

#### ***Carbla***

Alternating samples (d0, d2, d4, d6, d8) of the polar fraction (F4+5 from the five-fraction chromatography) of the Carbla ooids extracts were analyzed.

Highborne Cay TLE samples and Carbla FAME samples were sent to the NOSAMS Sample Preparation Lab at WHOI for radiocarbon analysis. The raw materials were combusted in evacuated quartz tubes with 100mg CuO and the resultant dioxide reacted with Fe catalyst to form graphite. The graphites were then analysed for  $^{14}\text{C}$

contents on the 500 kilovolt AMS system using NBS oxalic acid I (NIST-SRM-4990) the primary standard. Data were corrected using measured  $^{13}\text{C}/^{12}\text{C}$  ratios.

### ***Radiocarbon Dating of Ooid Carbonate***

The  $^{14}\text{C}$  age of the carbonate, which provides insight into the timescale of ooid formation and the age of these samples, was determined in collaboration with Steven Beaupre at WHOI. Using continuous-flow accelerator mass spectrometry (CFAMS), Dr. Beaupre developed a method to measure the  $^{14}\text{C}$  age of the ooid carbonate as a function of ooid radius. More details of this method are available in Beaupre 2013, in prep. Because this method is still in development, it is important not to infer too much from these data, but these preliminary results can allow us to further develop and refine our hypothesis regarding ooid formation.

Three sizes of sieved ooid samples from Highborne Cay were measured: <.250mm (only the largest, non-ooid material removed), between 0.177 and .250 mm, and .105 and .177 mm. One sieved ooid sample from Carbla was measured: between .590 and .250 mm

### ***Gas Chromatography-Mass Spectrometry (GC-MS) Analysis***

Samples were analyzed using an Agilent 7890A GC equipped with a Gerstel PTV injector and interfaced to an Agilent 5975 Mass Selective Detector. The GC was fitted with a J&W DB1-MS 60 m x .250 mm x .25  $\mu\text{m}$  capillary column using helium as the carrier gas. The oven was held at 60°C for 2 minutes, then the column ramped to 150°C at 10°C/min, then to 315° at 3°C/min for a total run time of 90 minutes. Peaks were identified by comparison of mass spectra to standard compounds when available, and library spectra, and retention time and order.

### ***Stable Isotope Ratio Mass Spectrometry (IRMS) Analysis***

Compound-specific  $^{13}\text{C}/^{12}\text{C}$  isotope results for lipids were obtained with a ThermoFinniganTraceGC equipped with a J&W DB-1MS column (60 m x 32 mm, 0.25 mm film). Chromatographic conditions were initially 60°C for three minutes, ramped from 60° – 180°C at 10°C/min, then 180° – 320°C at 40°C/min, and finally held at 320°C for 40 minutes. The GC was coupled to a combustion furnace interfaced to a Finnigan MAT DeltaPlus XP isotope ratio monitoring mass spectrometer operated with Isodat 2.0. Peaks were identified by comparison of retention order and relative height to GC–MS chromatograms. Samples were analyzed in triplicate.

Compound-specific D/H ratios of FAMES were measured at Caltech using methods based on previous studies of FAMES (Osburn et al., 2011). They were measured using a ThermoFinnigan Trace GC coupled to a DeltaplusXP isotope ratio mass spectrometer (IRMS) via a pyrolysis interface (GC-TC) operated at 1430°C. External FAME standards

were analyzed after every fifth sample. Each sample was injected using a PTV injector operated in splitless mode with solvent venting. A thick-film ZB-5 ms column (30 m long, 0.25 mm I.D., 1.00  $\mu$ m film) was used for isotope analysis with He carrier gas flow rate at 1.4 ml/min. The GC oven temperature was held at 100°C for 1 min, ramped at 20°C/min to 205°C, ramped at 0.8°C/min to 220°C, ramped at 8°C/min to 320°C and held for 10 minutes. Peaks were identified by comparison of retention order and relative height to GC–MS chromatograms. Isotope ratios were calculated using ISODAT NT 2.5 software by comparison to methane reference gas peaks as previously described (Wang and Sessions, 2008) and are reported in the standard  $\delta$ D notation ( $\equiv R_{\text{sample}}/R_{\text{std}} - 1$ ) as permil (‰) variations relative to the VSMOW standard. Samples were analyzed in triplicate where possible, however low sample abundance prevented this in some samples.

The H-isotopic composition of water collected from Carbla, Hamelin Pool was determined using a spectroscopic Water Isotope Analyser (Los Gatos Research, Inc). The single sample was analyzed five times against two working standards. Measured isotope ratios were converted to  $\delta$ D values by comparison with the two standards, and normalized to the SMOW-SLAP scale.

### ***Intact Polar Lipids (IPL) Analysis***

IPLs were analyzed without preceding sample clean-up on a Agilent 1200 series HPLC system coupled to an Agilent 6520 Accurate-Mass Quadrupole Time-of-Flight (QTOF) mass spectrometer with an electrospray ionization interface (ESI). Aliquots of total lipid extracts were dissolved in DCM:MeOH, 9:1 (v/v) and separation of compounds was achieved on a Waters Acquity UPLC BEH Amide column (2.1x150 mm) following the protocol after Wörmer et al., 2013. ESI source parameters were optimized to a drying gas temperature of 200°C, a drying gas flow of 6 L/min, nebulizer pressure of 40 psig, capillary voltage of 3000V and a fragmentor voltage of 175V. The QTOF was set to a scan mode of 400-2000 m/z in MS1 and 100-2000 m/z in MS2.

### ***Glycerol Dialkyl Glycerol Tetraethers (GDGTs) Analysis***

For GDGT analysis aliquots of the total lipid extract were dissolved in hexane/isopropanol, 99:1 (v/v) and subsequently analysed on an Agilent 1200 series HPLC systems coupled to and Agilent 6130 MSD single quadrupole via an APCI ion source, operated in positive mode. The compounds were separated on a Prevail Cyano colum (2.1 x 150 mm, 3mm Grace, Deerfiel, IL, USA) following the protocol of Liu et al., 2012. The APCI settings were set to a drying gas temperature of 350°C with a flow rate of 6 L min<sup>-1</sup>, nebulizer pressure of 30 psig, capillary voltage of 2000V, and corona current of 5 mA. The detector was set using Chemstation software (Agilent, version B.04.03) for selective ion monitoring (SIM) of [M+H]<sup>+</sup> ions after Liu et al., 2012 (Liu et al., 2012).



# Results

## Sieving

The size of the ooids from Highborne Cay is uniformly distributed with almost all of the ooid grains between .105 mm and .250 mm. Carbla ooids are slightly larger, with most grains between .177 mm and .540 mm. The single most abundant size fraction of ooids was used in the remaining experiments, which for Highborne Cay is ooids between .105 and .177 mm, and for Carbla is .177 and .250 mm.

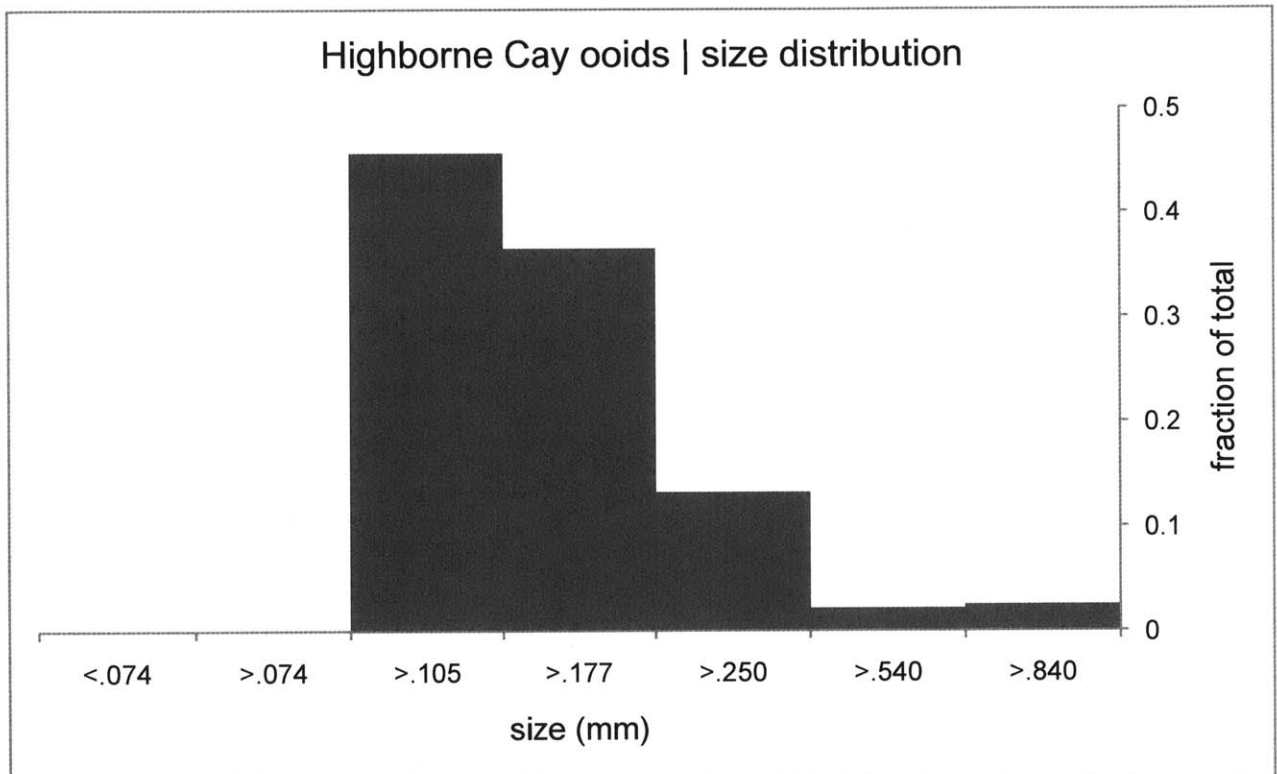


Figure 1: Size distribution of Highborne Cay ooids.

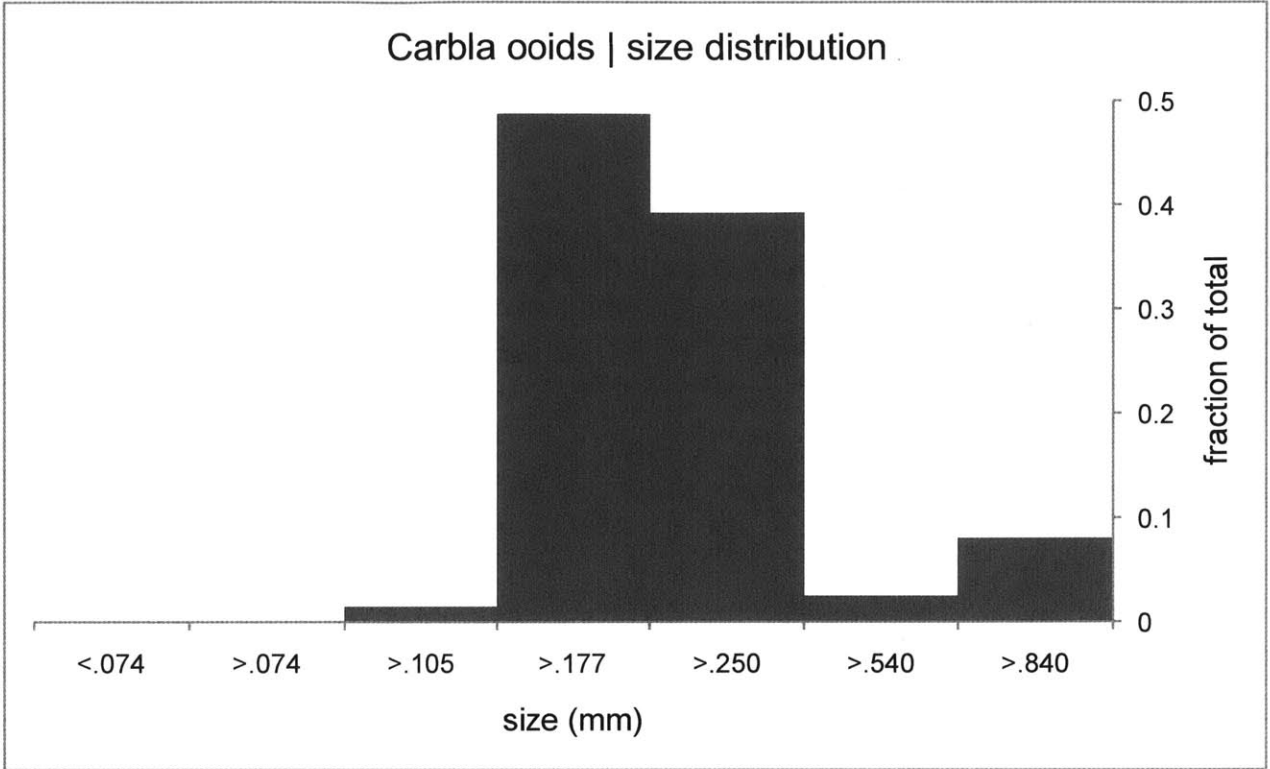


Figure 2: Size distribution of Carbla oids.

## Extraction

The weights of the extracts from the dissolution experiment are tabulated below. In the Highborne ooids, d0 yielded > 1 mg of material, but the other extracts were in the tenths of milligrams. This low yield was not enough to perform all of the analyses we hoped to; instead we focused on radiocarbon analysis of organic extract. The results of the Highborne experiment informed our decisions about the Carbla ooids; we increased the sample size and decreased the number of dissolutions. The Carbla ooids yielded ~1 mg of material in most of the extracts, which was enough to aliquot for the several analyses we wanted to perform, including radiocarbon analysis, lipid analysis, and stable carbon and hydrogen isotope analysis.

Sample	Highborne Ooids		Carbla Ooids	
	F1	F2	F1	F2
d0	1.88	0.17	0.32	0.58
d1	0.33	0.29	0.07	0.01
d2	0.34	0.29	1.62	66.03
d3	0.58	0.27	0.51	0.51
d4	0.47	0.33	1.38	na
d5	0.40	0.26	1.37	4.91
d6	0.28	0.27	1.51	10.09
d7	0.24	0.28	1.08	38.57
d8	0.32	0.26	1.82	9.60
d9	0.28	0.23	1.72	12.16
d10	na	na	0.99	4.16
d11	0.81	0.22		
d12	0.20	0.22		
d13	0.15	0.25		
d14	0.16	0.22		
d15	0.26	0.25		
d16	0.26	0.23		
d17	0.28	0.41		
d18	-0.08	0.19		
d19	0.29	0.13		
d20	na	na		

**Table 1: Sample weights of extracts from ooid dissolution experiments. Mass is listed in milligrams.**

### ***Elemental Sulfur***

The absence or presence, as well as a qualitative description of the amount of copper shot needed to remove all of the sulfur is tabulated below.

### ***Highborne Cay***

Sample	d0	d1	d2	d3	d4	d5	d6	d7	d8	d9	d10
Sulfur	0	0	0	0	0	0	0	0	***	0	na

Only sample d8 of the ten Highborne Cay samples that were analyzed contained elemental sulfur, and a lot of copper shot was required to remove it all. (Because these samples were quite organic lean, it is possible the other nine samples contained very small amounts of sulfur that was removed by the copper shot, but such a small amount of blackening occurred that it went unnoticed.)

### ***Carbla***

Sample	d0	d1	d2	d3	d4	d5	d6	d7	d8	d9	d10
Sulfur?	0	*	*	*	*	*	*	***	***	***	***

Elemental sulfur was present in almost all of the extracts from Carbla ooids. There was no sulfur in the extract of the Carbla ooid biofilm (d0), a little sulfur in the first six dissolutions (d1 through d6), and a lot of sulfur in the final four dissolutions (d7 through d10).

## Radiocarbon Dating of Organic Matter

### Highborne Cay

The age of the organic matter extracted from ooids from Highborne Cay vary in age between 955 years (err = 30) and 5,790 years (err = 70) in an unsystematic pattern.

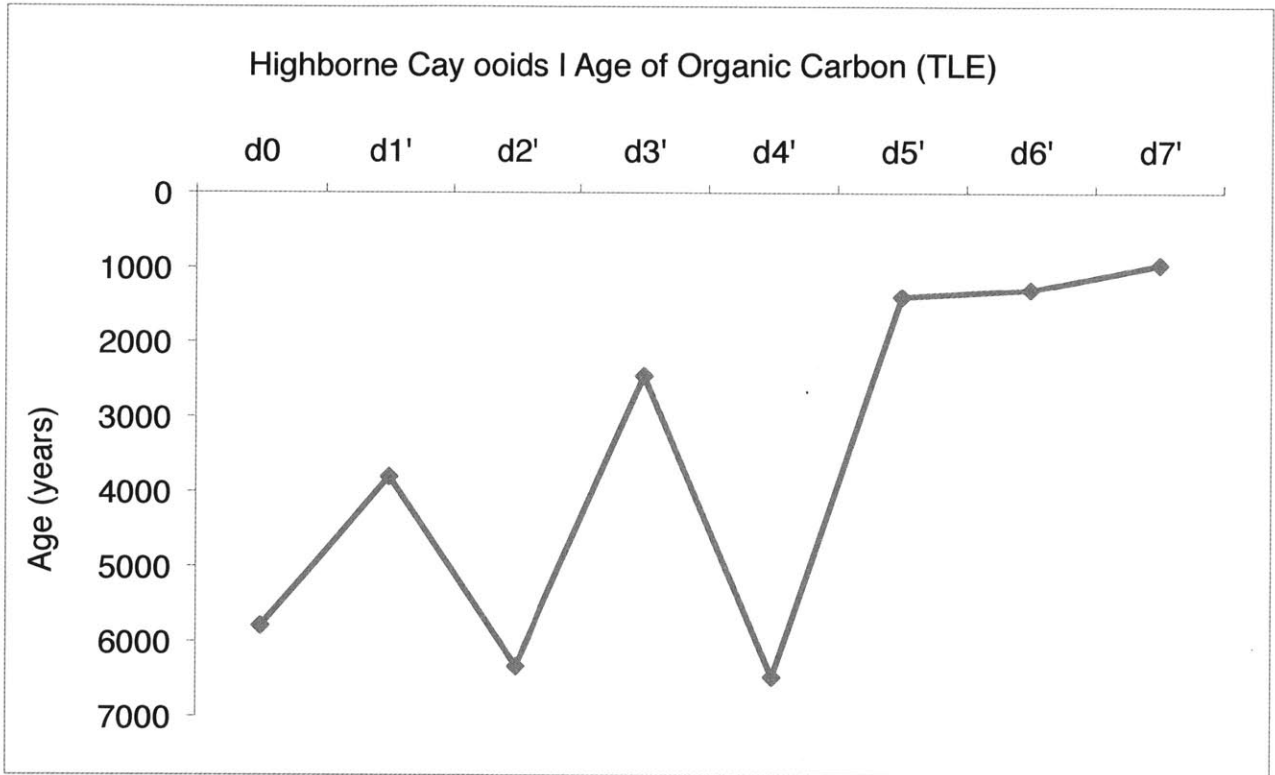
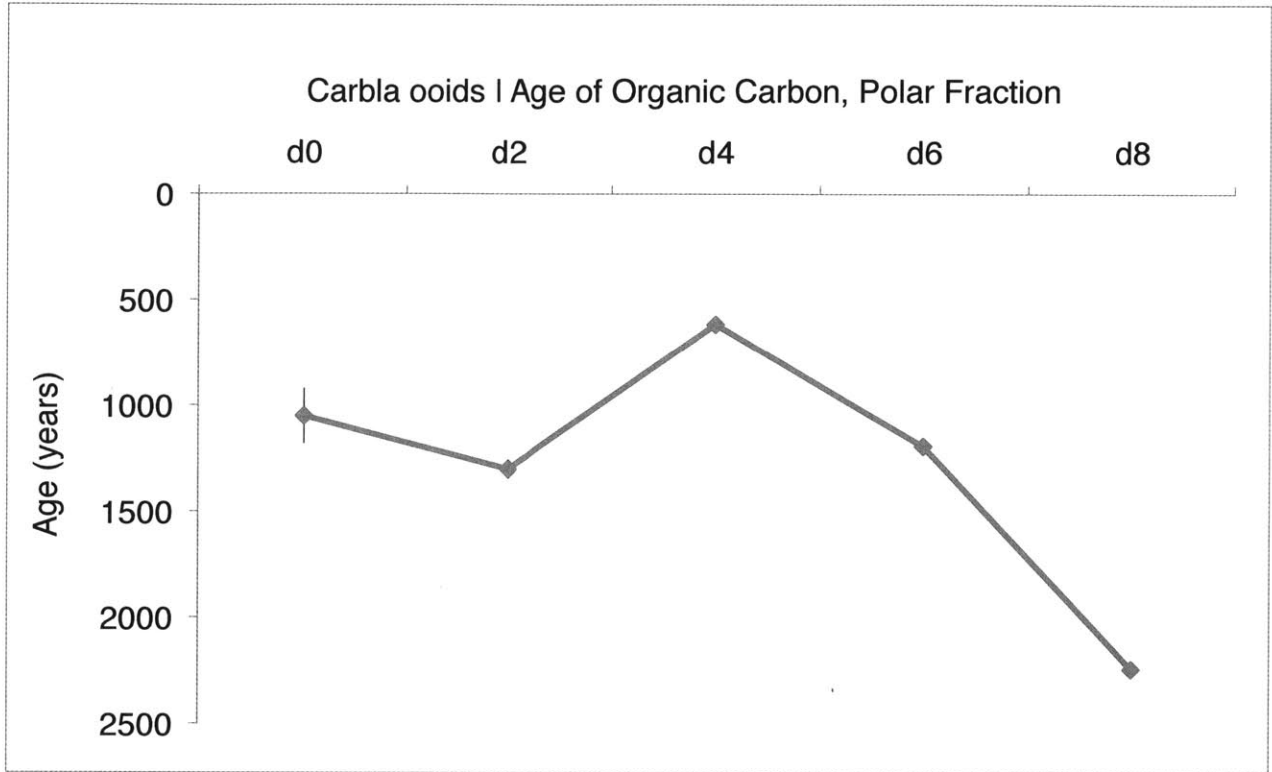


Figure 3: Radiocarbon age of TLE from Highborne Cay ooids. Extract d1' through d7' represent clumped, adjacent samples from the original extracts d1 through d20. Error bars are  $2\sigma$  confidence intervals on the radiocarbon age (not visible because they are smaller than the size of the marker).

*Carbla*

The age of the polar fraction (fractions 4 and 5 from the 5-Fraction column chromatography) from ooids from Carbla vary in age from 1,050 years (d0; err = 130) to 2,240 years (d8; err = 35), with the youngest value from sample d4 (615 years, err = 25).



**Figure 4: Radiocarbon age of polar fraction of the organic extracts from Carbla ooids dissolution experiment. Error bars are 2σ confidence intervals on the radiocarbon age.**

## Radiocarbon Dating of Ooid Carbonate

### Highborne Cay

The results are shown in Figure 5 on a plot of age versus mean spherical radius. The largest ooids are approximately 300 years old, and as the radius decreases from acid dissolution, the general trend is for the age to increase. At the end of the experiment, when the radius is approximately 50  $\mu\text{m}$ , the  $^{14}\text{C}$  age is  $\sim 1,000$  years.

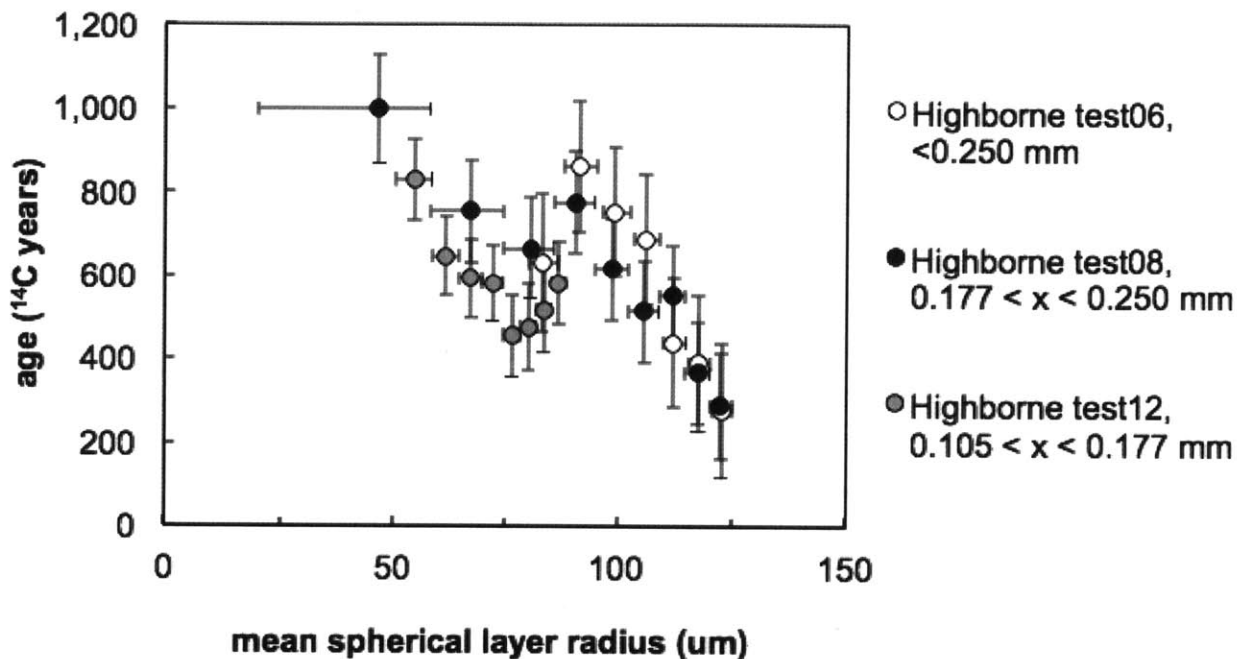


Figure 5: Age of Highborne Cay ooids carbonate versus ooid radius, based on radiocarbon analysis. Three sieved size fractions were measured. Data are courtesy of Dr. Beaupre, NOSAMS.

## Carbla

The largest Carbla ooids have a  $^{14}\text{C}$  age of  $\sim 200$  years, and get older with decreasing ooid radius. In the last data point was taken when  $\sim 60\%$  of the carbonate was dissolved; when the ooid radius reached  $\sim 125$   $\mu\text{m}$ , the  $^{14}\text{C}$  age of the released carbonate is  $\sim 1,250$  years. A line was fit to the data using a geometric mean least squares regression model.

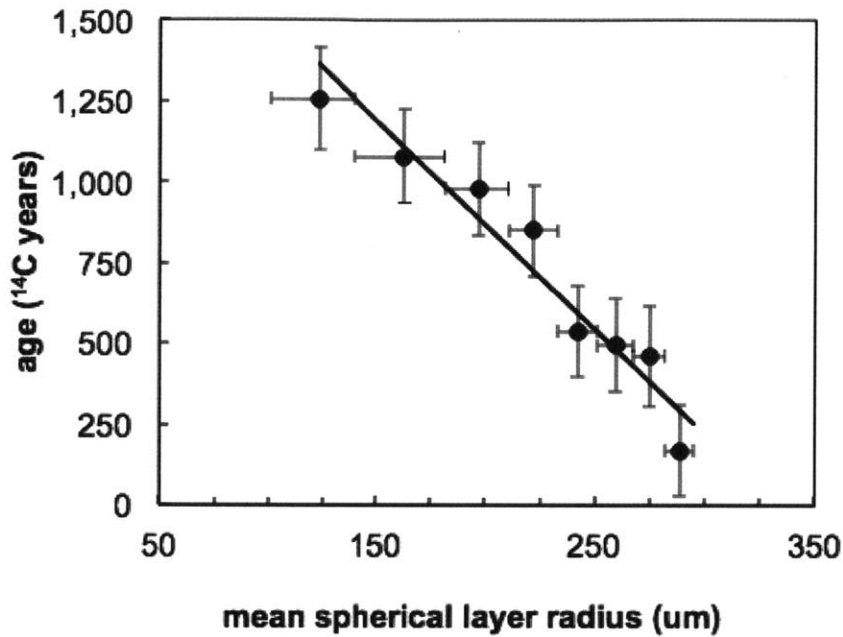


Figure 6: Age of Carbla ooids carbonate versus ooid radius, based on radiocarbon analysis. Data are courtesy of Dr. Beaupre, NOSAMS.



## ***Lipid distribution***

The FAMES fraction of the freely extractable lipids (d0 extract) of the Carbla ooids contained saturated, straight chain (normal, or n) FAMES with chain lengths from C=14 to C=28; the dominant compound is n-C16, followed by n-C18, which are the most common fatty acids in bacterial and eukaryotic cell membranes. The normal FAMES exhibit a pronounced even-over-odd carbon number predominance. There are short (C=15-17) branched (iso, anteiso, and 10-methyl) FAMES. There were also compounds that precede the long (C=19 to C=28), saturated straight chain FAMES that, based on retention time and comparison of spectra to library, we conclude are fatty ketones. There were two large peaks, marked by asterisks, that appear to be contaminants.

The matrix bound lipids of the Carbla ooids (extracts d2 through d10) contain many of the same compounds as the biofilm (d0). A more detailed description of each sample follows:

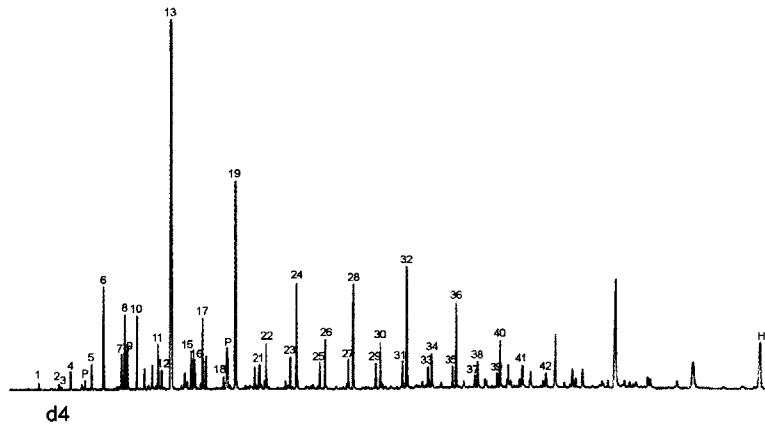
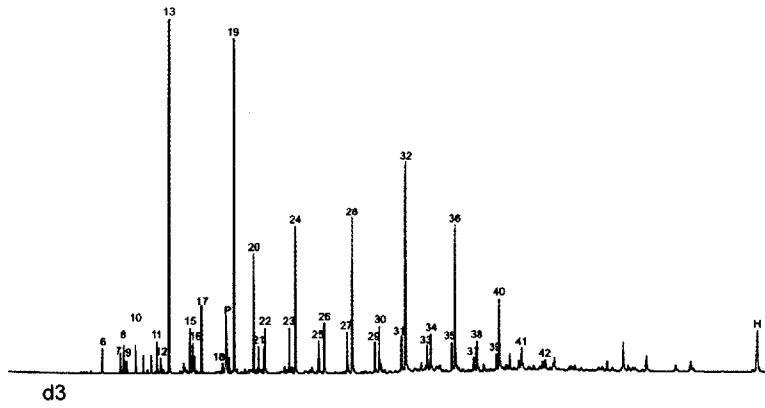
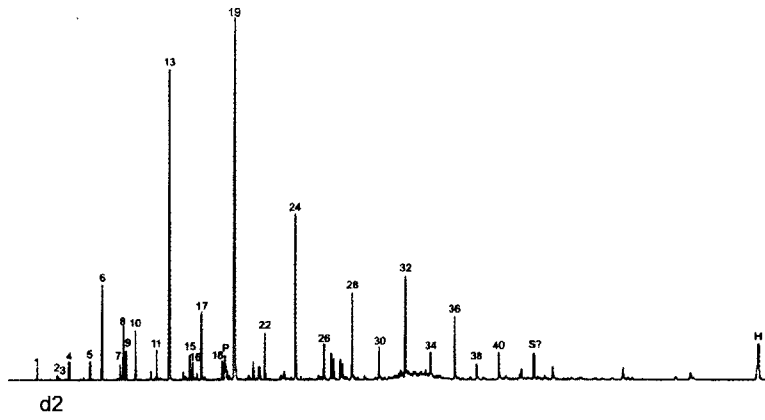
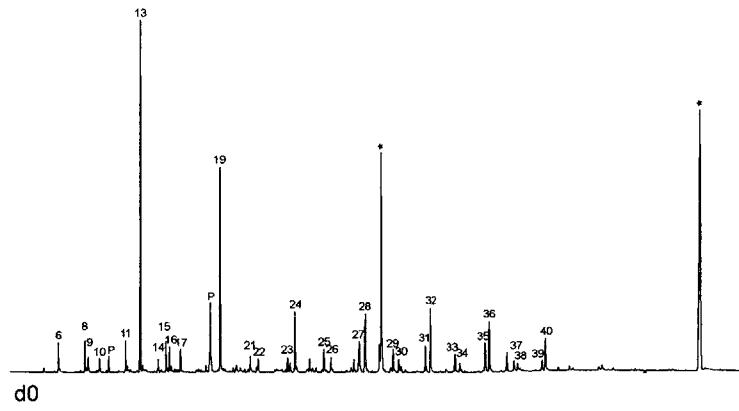
In d2, the most abundant FAME is n-C18, followed by n-C16. There is an even-over-odd pattern, and have chain lengths from C=12 to C=30. There are small amounts of branched FAMES with 16, 17, and 18 carbons including iso, anteiso, and 10-Me branch patterns. There is also a late eluting peak (rt~80 min) that we conclude to be a derivative of homohopanoic acid.

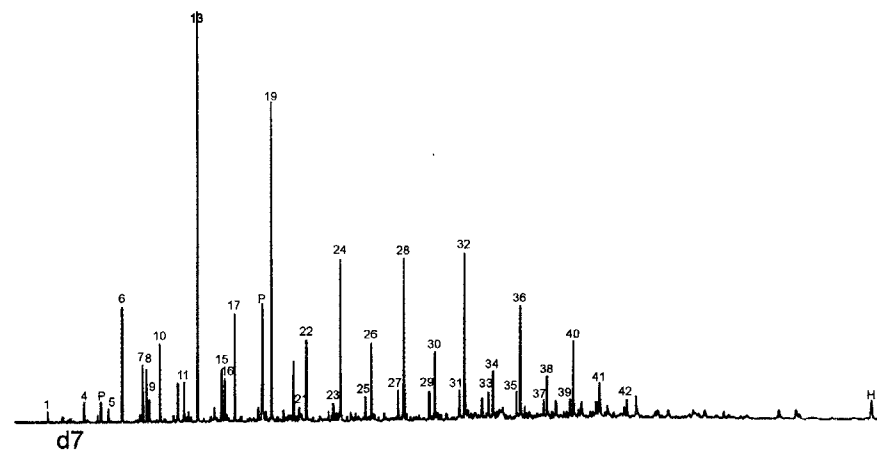
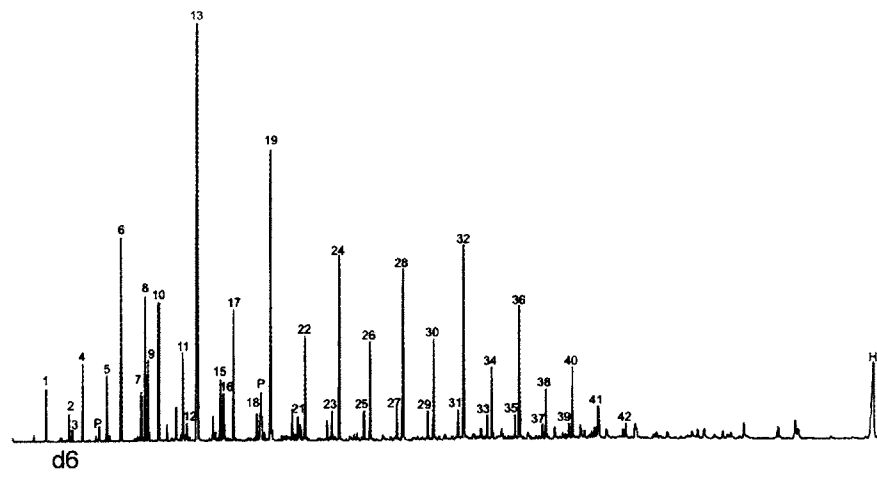
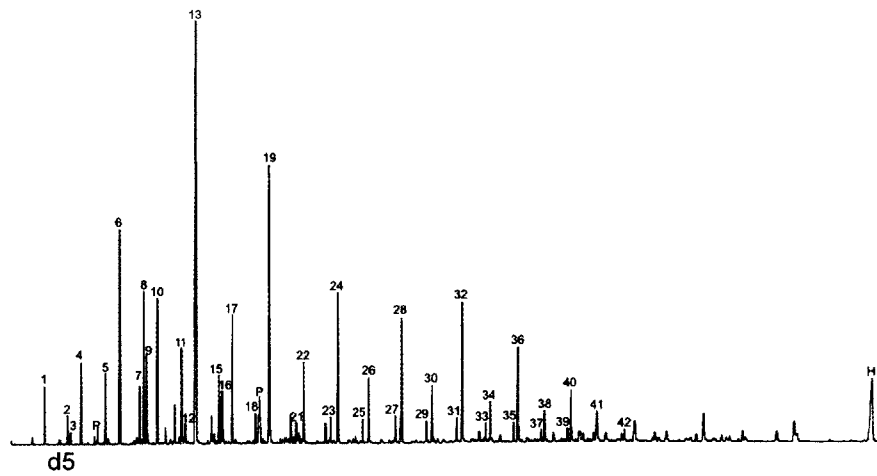
In d3, n-C16 and n-C18 FAME are the two predominant peaks and are nearly equal in abundance; their relative abundance is less than in d2. The even-over-odd predominance continues in the normal FAMES and includes the same chain lengths seen in d2 (C=12 through 30). In this sample, all of the normal FAMES include a small doublet peak that appears to be a fatty ketone. The ketones have a slight even-over-odd pattern but are roughly the same size as each other. The homohopanoic acid-ME is present.

In d4, n-C16 is the most abundant FAME, followed by n-C18 and the rest of the even carbon number FAMES. There are also the branched medium chain length (15,16,17,18FAMES as seen in the previous samples. The corresponding ketones are also present, as they are in d3. The same late eluting homohopanoic acid is present.

Samples d5 and d6 shares a lot of the same characteristics as the other samples (n-C16 and 18 are the most abundant, branched FAMES, even-over-odd predominance, corresponding ketones, homohopanoic acid derivative), but with more small (C=12-16) compounds including branched, possibly unsaturated FAMES.

Sample d7 is very similar to d4, except it does not contain a significant amount of homohopanoic acid ME. Sample d8 is very similar to d5 and 6. It is one of the few samples that does not contain corresponding ketones, however. Samples d9 and d10 shares many characteristics with d8, including the abundant branched FAMES. d9 has a small hump of unresolved material around C=24.





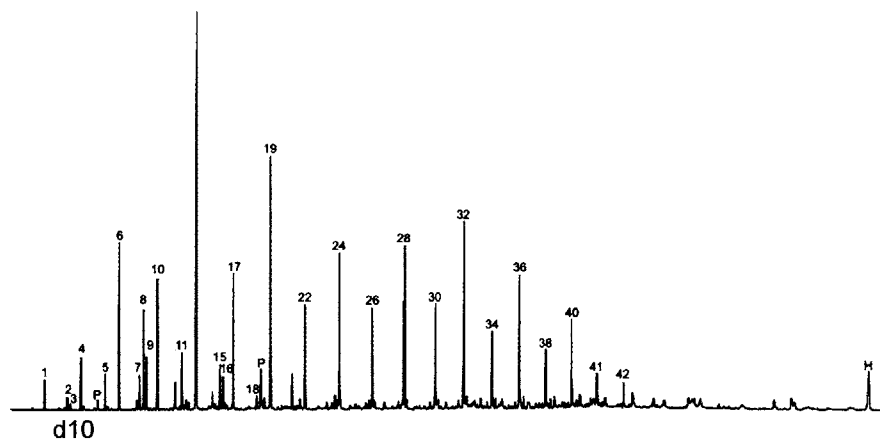
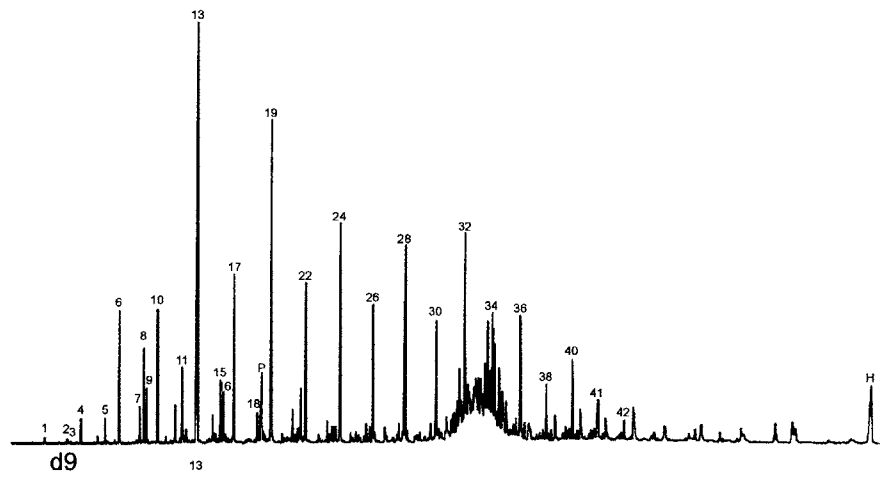
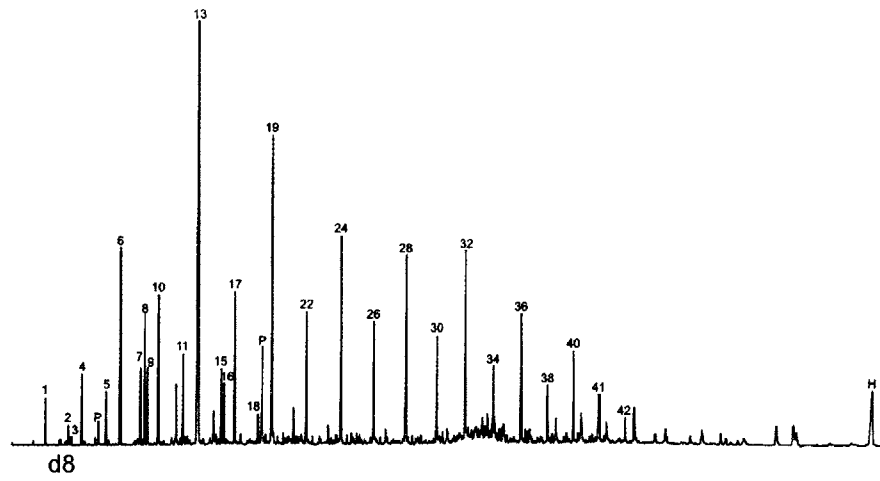


Figure  
dissolution of Carblā ooids. Numbers correspond to compounds on Tables 2 and 3.

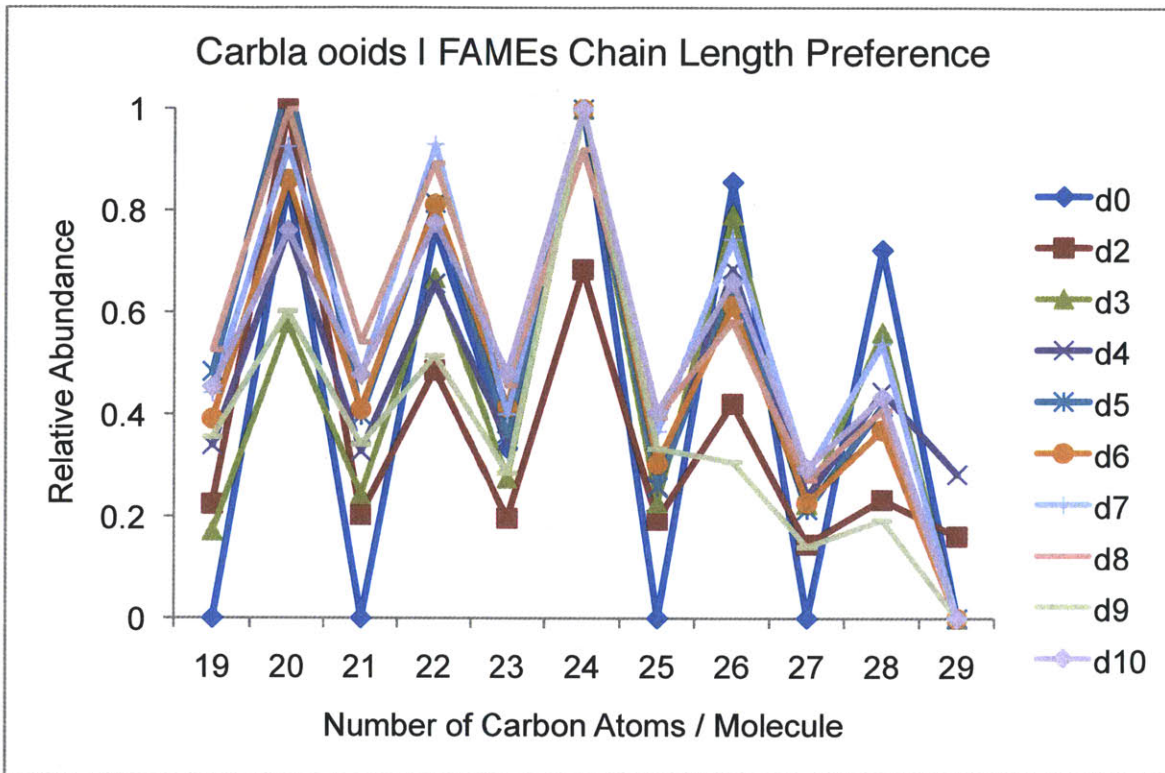


Figure 8: Chain length preference of FAMES from Carbla ooids. There is a clear even-over-odd pattern.

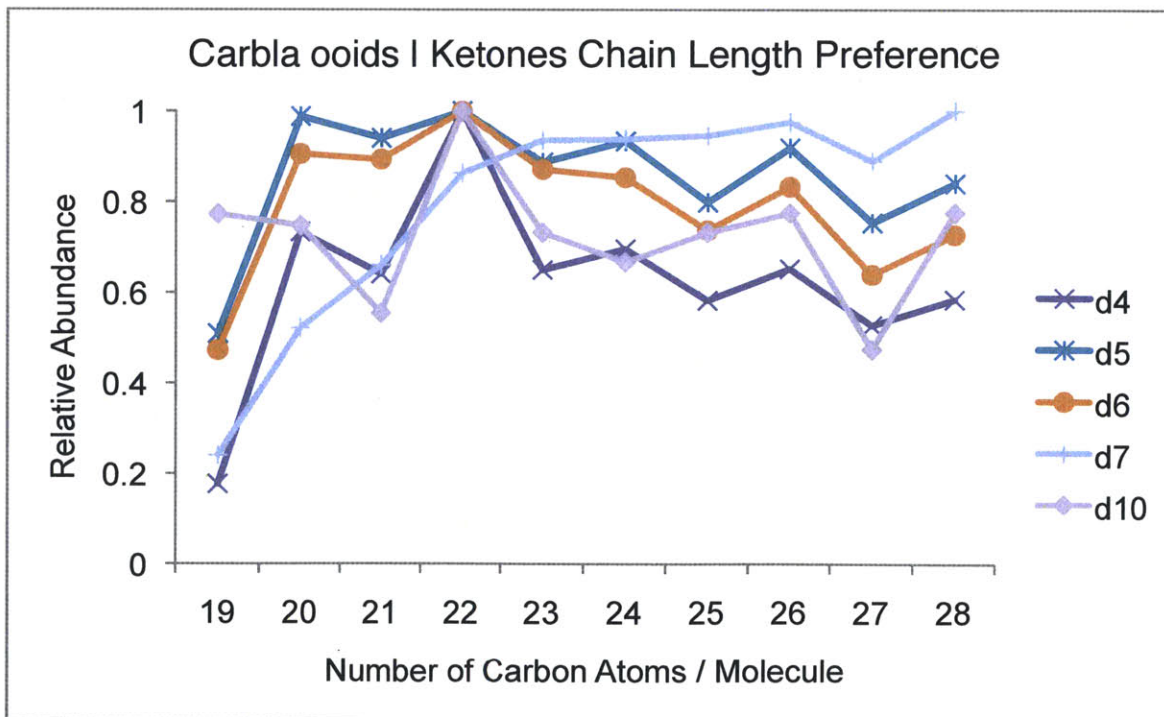


Figure 9: Chain length preference of ketones from Carbla ooids. The even-over-odd preference is not as pronounced as the FAMES.

Table 2: Compound specific stable carbon (<sup>13</sup>C) isotope values of Caribba ooid dissolution extracts.

Number	Compound	$\delta^{13}\text{C}$ (PDB ‰)									
		d0	d2	d3	d4	d5	d6	d7	d8	d9	d10
1	n-C12 FAME		-20.44		-13.22	-13.97	-13.57	-15.53	-14.25	-13.36	-13.71
2	iso-C13 FAME										
3	ai-C13 FAME										
4	n-C13 FAME		-13.81		-12.68	-13.33	-12.65	-16.73	-14.59	-13.30	-14.50
5	iso-C14 FAME		-14.87		-13.96	-13.94	-13.61	-12.92	-13.71	-13.49	-12.33
6	n-C14 FAME	-21.58	-17.81	-13.01	-17.06	-16.05	-15.44	-17.04	-16.17	-15.88	-15.02
7	10 Me-C15 FAME		-17.81	-18.29	-20.16	-16.78	-16.34	-16.13	-16.49	-16.43	-15.29
8	iso-C15 FAME	-15.02	-13.91	-12.32	-12.60	-13.17	-12.54	-12.54	-12.92	-13.19	-12.05
9	ai-C15 FAME		-14.02		-13.14	-13.38	-12.50	-13.80	-13.17	-13.71	-12.28
10	n-C15 FAME	-20.16	-15.66	-15.18	-15.98	-15.07	-14.62	-15.24	-15.60	-15.66	-14.24
11	iso-C16 FAME	-18.70	-14.51	-16.57	-15.55	-14.53	-15.12	-16.49	-14.47	-15.29	-14.20
12	n-C16 alkan-2-one										
13	n-C16 FAME	-22.62	-19.87	-16.70	-22.23	-17.38	-16.65	-17.36	-17.30	-17.40	-16.50
14	10 Me-C17 FAME										
15	iso-C17 FAME	-15.55	-16.31		-16.45	-16.54	-16.73	-17.09	-17.76	-17.68	-17.12
16	ai-C17 FAME	-17.86	-16.20		-16.29	-15.14	-13.93		-15.51	-15.24	-14.86
17	n-C17 FAME	-18.19	-15.62	-13.74	-14.56	-14.25	-14.32	-15.02	-15.52	-16.90	-15.31
18	iso-C18 FAME										
19	n-C18 FAME	-23.22	-24.88	-17.09	-20.32	-16.02	-15.95	-16.79	-16.72	-17.39	-16.32
20	n-C18:1 FAME										
21	n-C19 alkan-2-one		-27.77		-30.78	-15.37	-22.57	-15.96	-13.78	-15.05	-19.30
22	n-C19 FAME		-16.19	-13.96	-15.18	-15.54	-16.18	-17.01	-17.62	-17.85	-17.05
23	n-C20 alkan-2-one	-24.50		-13.91	-15.41	-15.62	-17.60	-24.76		-18.18	-18.27
24	n-C20 FAME	-21.90	-22.15	-14.89	-15.47	-14.72	-15.18	-16.90	-16.80	-17.48	-16.89
25	n-C21 alkan-2-one	-20.81	-30.59	-21.61	-23.41	-19.42	-25.82	-19.82		-18.20	-28.41
26	n-C21 FAME		-19.39	-17.52	-18.53	-18.84	-18.93	-20.33	-19.65	-20.23	-20.10
27	n-C22 alkan-2-one	-28.60		-20.56	-21.53	-20.83	-22.77	-24.49		-20.09	-26.19
28	n-C22 FAME	-21.75	-20.15	-17.46	-18.13	-18.45	-18.55	-19.20	-19.55	-20.06	-19.92
29	n-C23 alkan-2-one	-21.46		-21.24	-24.42	-24.13	-24.38	-22.20	-20.22	-16.41	-32.03
30	n-C23 FAME	-23.72	-23.87	-19.82	-20.13	-20.78	-20.19	-25.14	-20.45	-21.31	-20.31
31	n-C24 alkan-2-one	-21.89	-28.60	-23.94	-23.05	-24.37	-23.85	-25.44	-32.81	-25.94	-19.71
32	n-C24 FAME	-21.63	-19.84	-17.39	-17.73	-18.13	-18.49	-19.91	-20.35	-23.68	-19.69
33	n-C25 alkan-2-one	-20.93		-19.79	-20.44	-19.48	-19.86	-20.21	-26.42	-27.69	-17.60
34	n-C25 FAME		-20.33	-18.59	-19.13	-18.98	-18.74	-20.41	-21.30	-26.23	-20.15
35	n-C26 alkan-2-one	-24.53		-20.04	-20.04	-20.58	-20.07	-20.50		-14.61	-20.21
36	n-C26 FAME	-22.60	-18.65	-18.12	-18.55	-18.77	-18.56	-19.74	-19.84	-20.25	-19.84
37	n-C27 alkan-2-one			-21.15	-22.52	-25.27	-19.94	-22.86		-22.24	-20.55
38	n-C27 FAME		-20.80	-17.23	-19.01	-19.24	-18.51	-21.39	-19.75	-19.73	-19.86
39	n-C28 alkan-2-one	-23.66		-19.69	-19.80	-20.15	-20.15	-20.23	-22.33	-19.15	-18.79
40	n-C28 FAME	-22.30	-18.76	-17.27	-17.80	-17.84	-18.39	-19.59	-19.78	-20.37	-19.91
41	n-C29 FAME		-28.97		-22.90						
42	n-C30 FAME										
H	bishomohopanoic acid ME		-16.75	-15.25	-15.69	-16.42	-15.57	-14.39	-16.19	-16.48	-16.35

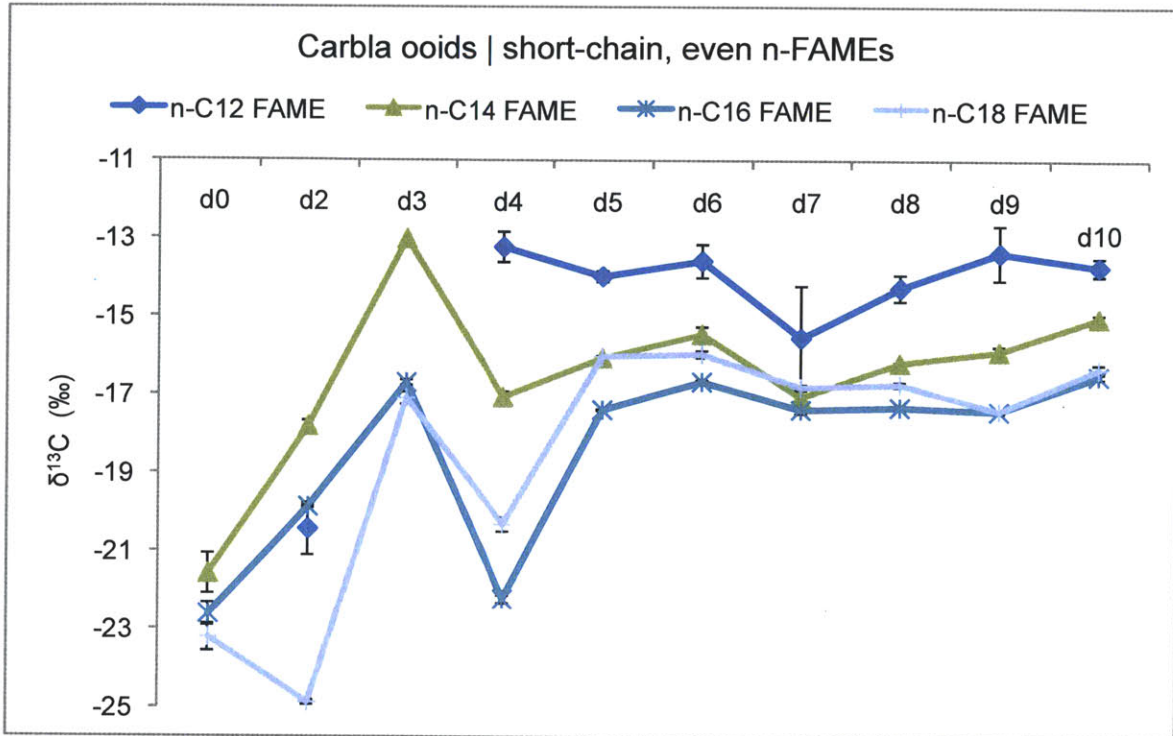


Figure 10: Carbon isotope values of short-chain, even carbon number, normal FAMES from Carbla ooids. Error bars are 2 standard deviations from triplicate analyses.

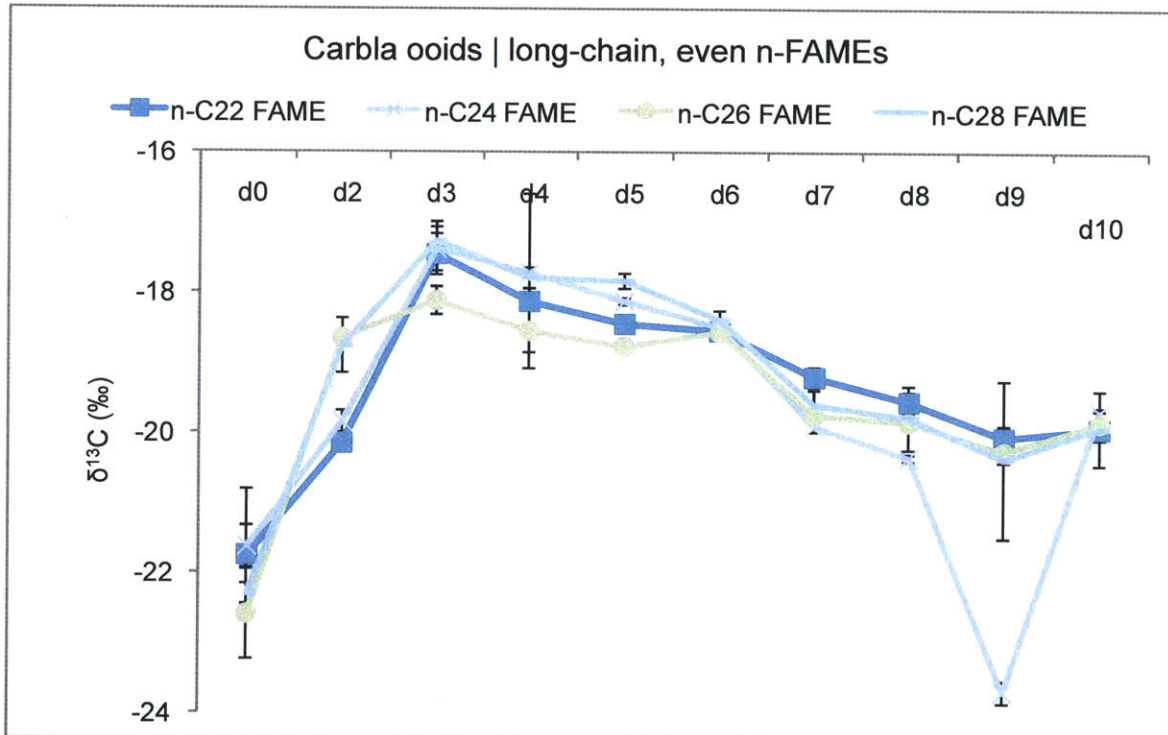


Figure 11: Carbon isotope values of long-chain, even carbon number, normal FAMES from Carbla ooids. Error bars are 2 standard deviations from triplicate analyses.

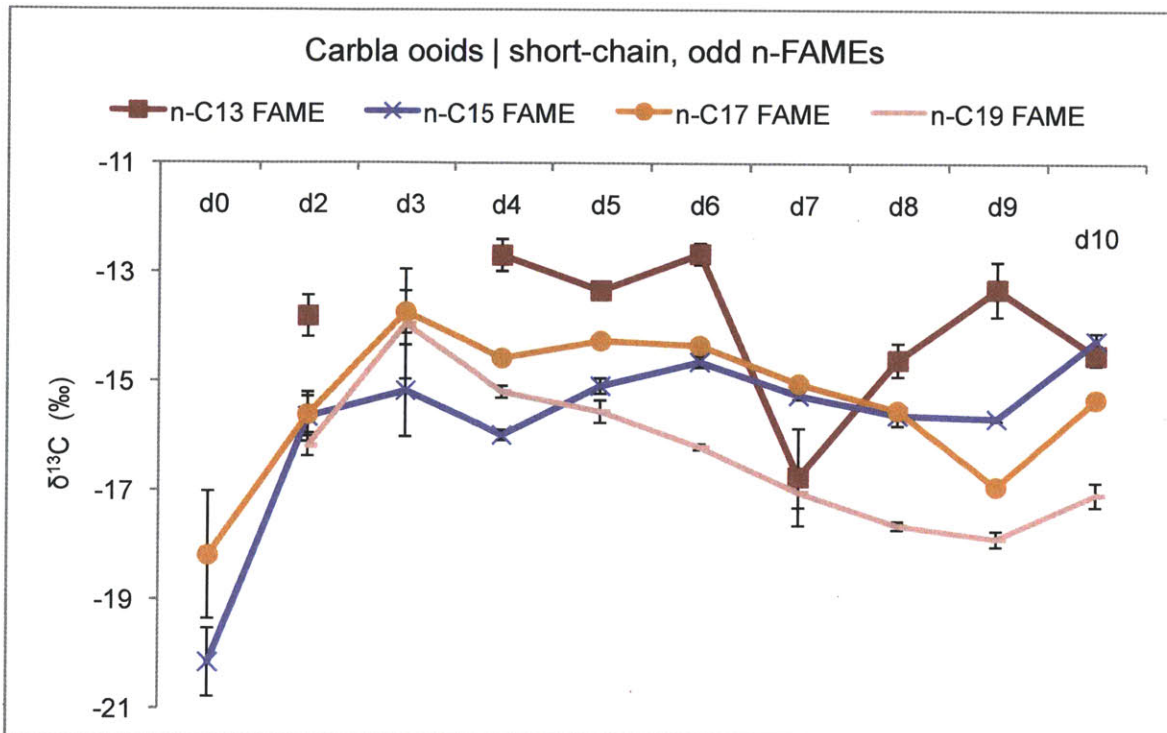


Figure 12: Carbon isotope values of short-chain, odd carbon number, normal FAMES from Carbla ooids. Error bars are 2 standard deviations from triplicate analyses.

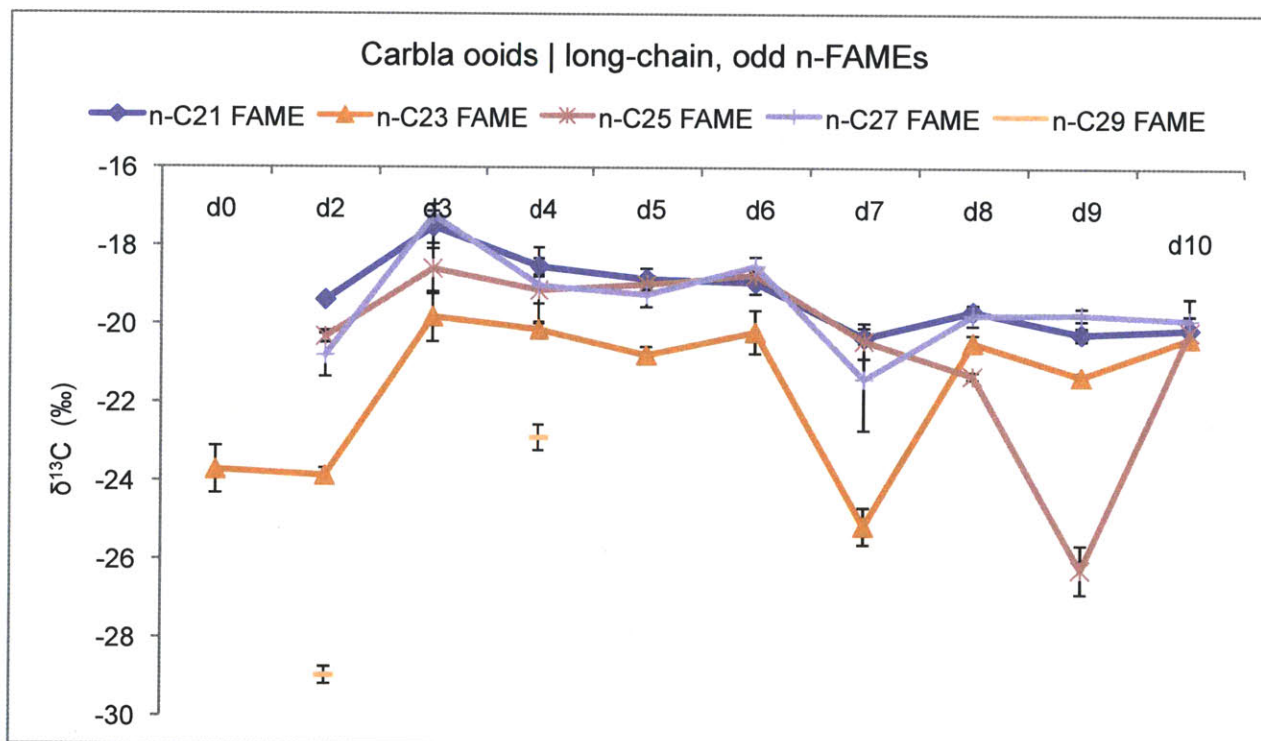


Figure 13: Carbon isotope values of long-chain, odd carbon number, normal FAMES from Carbla ooids. Error bars are 2 standard deviations from triplicate analyses.



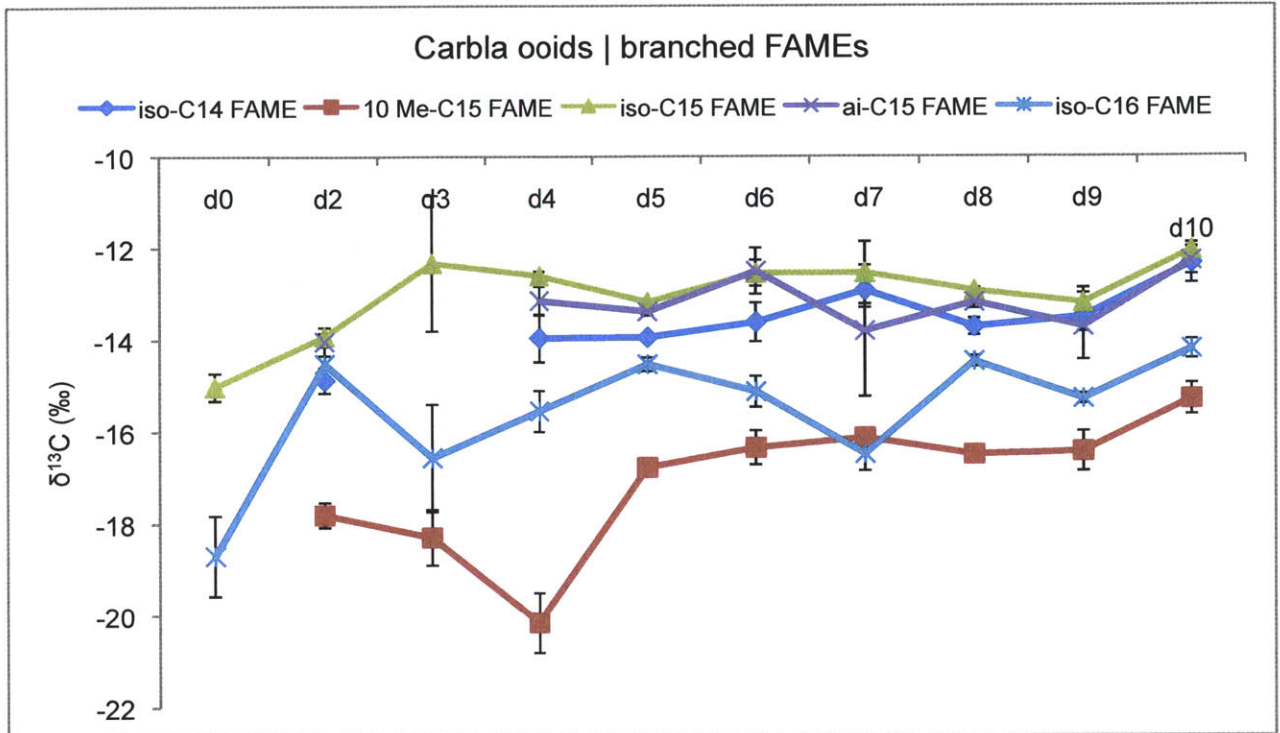
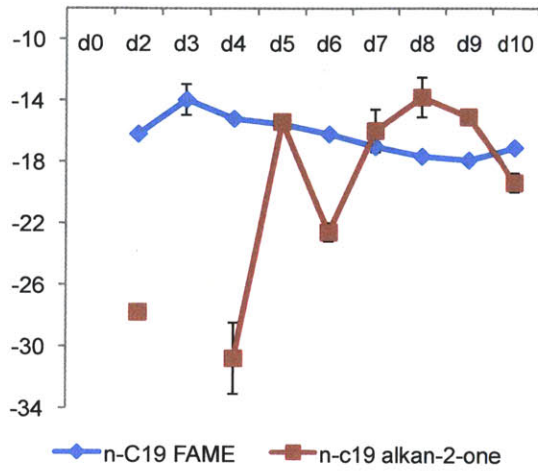
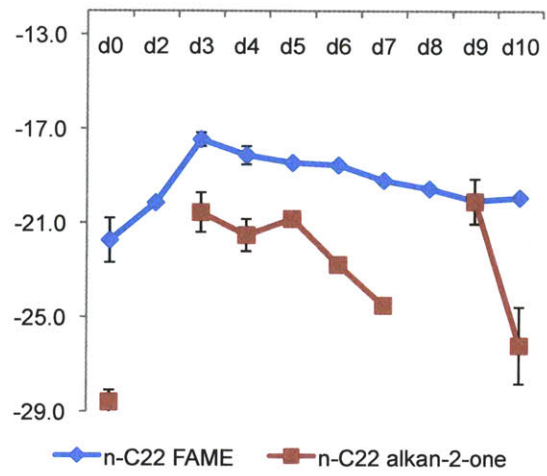


Figure 14: Carbon isotope values of branched FAMES from Carbla ooids. Error bars are 2 standard deviations from triplicate analyses.

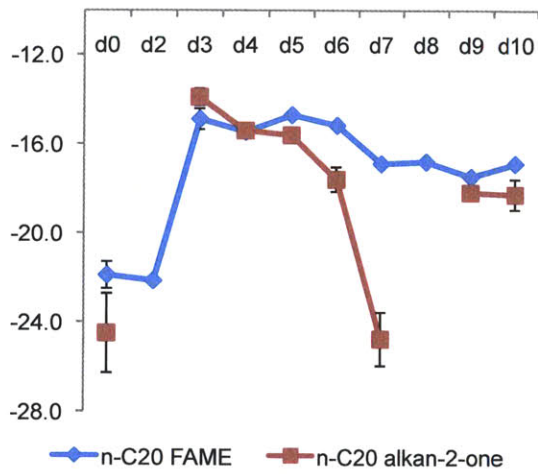
Carbla ooids | C19 Compounds



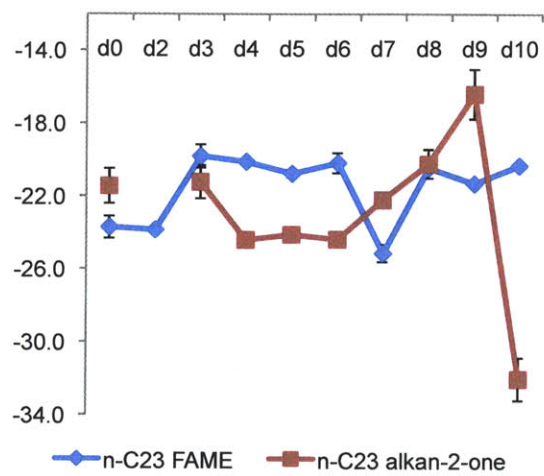
Carbla ooids | C22 Compounds



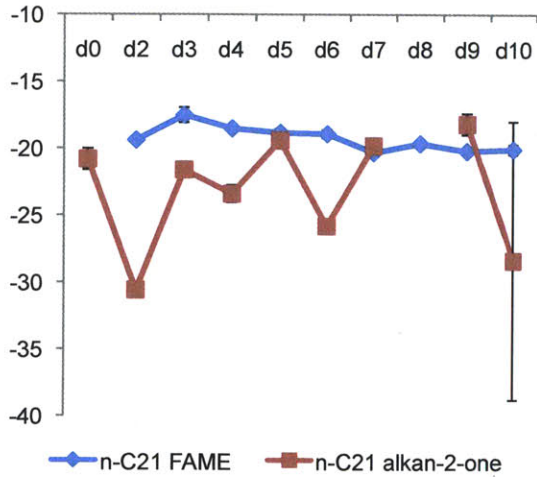
Carbla ooids | C20 Compounds



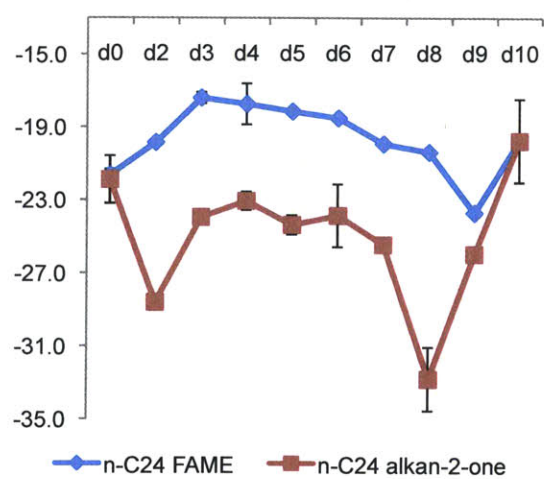
Carbla ooids | C23 Compounds



Carbla ooids | C21 Compounds



Carbla ooids | C24 Compounds



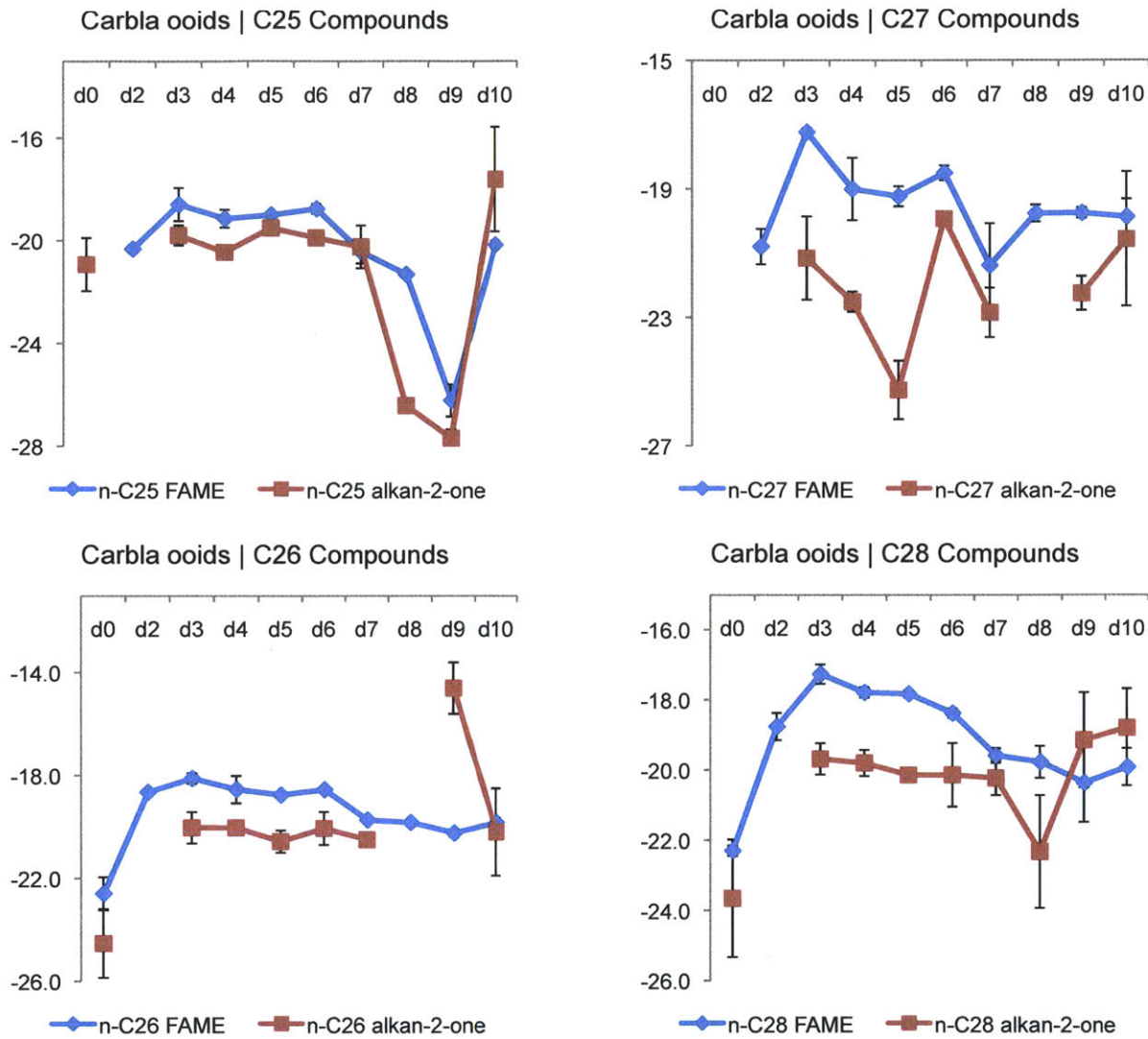


**Figure 15: A comparison of the carbon isotope values of FAMES and ketones with the same carbon number. Error bars are 2 standard deviations from triplicate analyses.**

## ***Stable Carbon Isotopes***

### *Straight Chain Saturated FAMES*

The results of the stable carbon isotope analysis of the Carbla ooid FAMES are tabulated (see Table 2). Most of the compounds have  $\delta^{13}\text{C}$  values between -12‰ and -30‰. The short chain, even carbon number, normal FAMES (n-C12 through n-C18) vary between -25‰ and -13‰ (See Figure 10). The exterior extract (d0) is ~-22‰, and then the compounds become heavier, stabilizing in d5 through d10 with values between approximately -18‰ and -14‰. The long chain, odd carbon number normal FAMES (n-C22 through n-C28) have similar  $\delta^{13}\text{C}$  values in each sample, but vary throughout the dissolution extracts (See Figure 11). The exterior has the lightest values (~-22‰), which then increase in samples d2 and d3 to a maximum of ~-18‰, then slowly decrease from d3 to d10 to about -20‰. The short chain, odd carbon number, normal FAMES (n-C13 through n-C19) display a similar pattern as the short chain, even carbon number, normal FAMES, but with more variability (especially in the compounds with lowest abundance i.e. n-C13) (See Figure 12). The long chain, odd carbon number, normal FAMES (n-C21 through n-C29) are absent from d0, but are fairly stable through samples d2 through d10, with values between -18‰ and -21‰ (See Figure 13). There are a few exceptions that appear to be outliers, which produce lighter  $\delta^{13}\text{C}$  values e.g. n-C29 in d2 is -29‰.

### *Branched FAMES*

The branched (iso-, anteiso-, and 10-methyl) short chain (C=14-16) FAMES measured in the samples have  $\delta^{13}\text{C}$  values between -12‰ and -20‰ (See Figure 14). Unlike the straight chain saturated FAMES, there is not a broad trend that overlies the data; they remain fairly consistent throughout the dissolution extracts, with some variability, especially in samples d0 through d4.

### *Long Chain Ketones*

In many samples, the enigmatic fatty ketones were abundant enough to determine their  $\delta^{13}\text{C}$  values. There is a lot of variability in  $\delta^{13}\text{C}$  values of the ketones, even between like compounds, ranging from -13‰ to -32‰. Plots of ketones and straight chain FAMES were made to determine if there is a relationship between the two types of compounds (see Figure 15). In general, the ketones seem to be slightly lighter than their corresponding FAMES, but this is not always the case. Although some sets of compounds track each other closely, such as C25 compounds, this is the exception, rather than the rule. The ketones are much more variable than their FAME counterparts, and it is unclear if they are related based on their stable carbon isotopes. Some of this variability may be due to their smaller abundance, making a measurement

more difficult. However, the variability between triplicate runs, shown in the error bars, is not particularly large for most ketones.

**Table 3: Compound specific stable hydrogen ( $^2\text{H}$  or D) isotope values of Carbia ooid dissolution extracts.**

Number	Compound	$\delta^2\text{H}$ (VSMOW ‰)									
		d0	d2	d3	d4	d5	d6	d7	d8	d9	d10
4	n-C14 FAME					-151.17	-144.62		-148.35	-146.61	-139.53
6	iso-C15 FAME					-52.26				-54.62	
7	ai-C15 FAME					-116.06					
8	n-C15 FAME					-141.32	-134.82		-129.39	-140.55	-135.69
9	iso-C16 FAME					-77.77				-81.59	
10	n-C16 FAME		-159.43	-183.77	-129.57	-132.54	-139.08	-132.81	-118.97	-132.87	
11	n-C17 FAME				-140.03	-131.31	-128.95	-136.97	-133.29	-133.54	
12	n-C18 FAME		-147.95	-136.22	-121.66	-117.95	-114.67	-114.82	-102.01	-113.59	
14	n-C19 FAME				-131.85				-126.40	-121.65	
16	n-C20 FAME		-156.22	-142.33	-138.32	-137.72	-129.29	-132.37	-133.63	-132.36	
18	n-C21 FAME				-145.57						
20	n-C22 FAME		-125.67		-106.33	-113.06	-120.46	-118.49		-121.65	
24	n-C24 FAME		-131.40		-118.42	-121.27	-129.45			-128.67	
28	n-C26 FAME		-112.52		-100.35		-115.30		-110.90	-119.64	

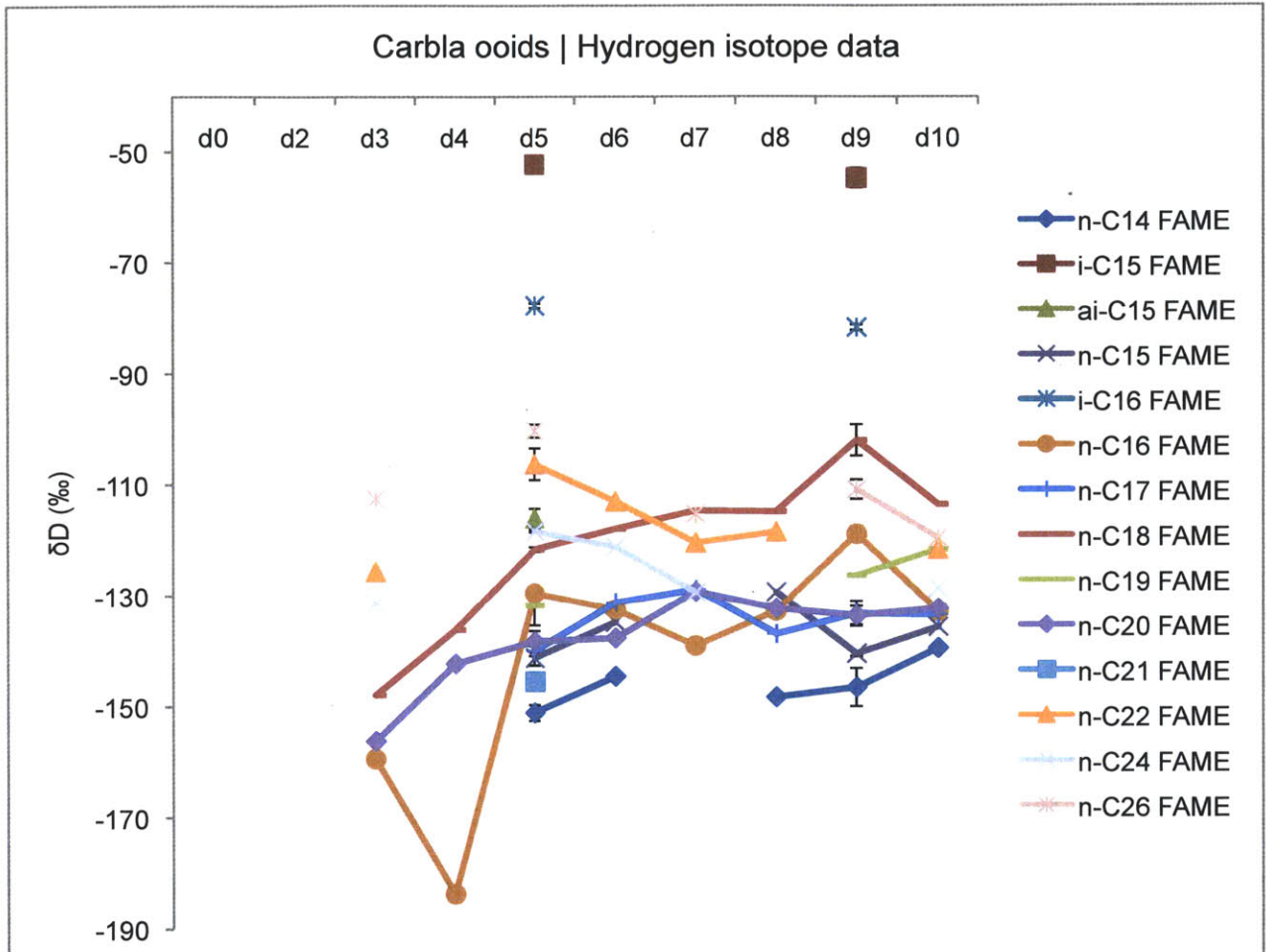


Figure 16: Compound specific stable hydrogen ( $^2\text{H}$  or D) isotope values of Carbla ooid dissolution extracts. Error bars, where present, are 2 standard deviations from replicate analyses.

## **Stable Hydrogen Isotopes**

### *Lipids*

Hydrogen isotope data was obtained for Carbla ooid samples with sufficient organic matter. The results are summarized in Table 3. The limited data set displays the same patterns as seen in previous work (Summons et al., Under Review): the iso- compounds are strongly enriched relative to normal (and one anteiso) FAMEs. Normal FAMEs have  $\delta D$  values between  $-150\text{‰}$  and  $-100\text{‰}$ , which do not vary systematically between samples d3 and d10. Iso-C15 has  $\delta D$  values of  $\sim -53\text{‰}$  in both d5 and d9, the two samples in which isotope data was obtained. Iso-C16 has  $\delta D$  values of  $\sim -80\text{‰}$  in the sample two samples. Unfortunately, the exterior sample (d0) was contaminated during sample preparation for the analysis, so we cannot compare the external and the internal  $\delta D$  values at this time.

### *Water*

The water from Hamelin Pool, near Carbla beach has a  $\delta D$  value of  $+14\text{‰}$ .

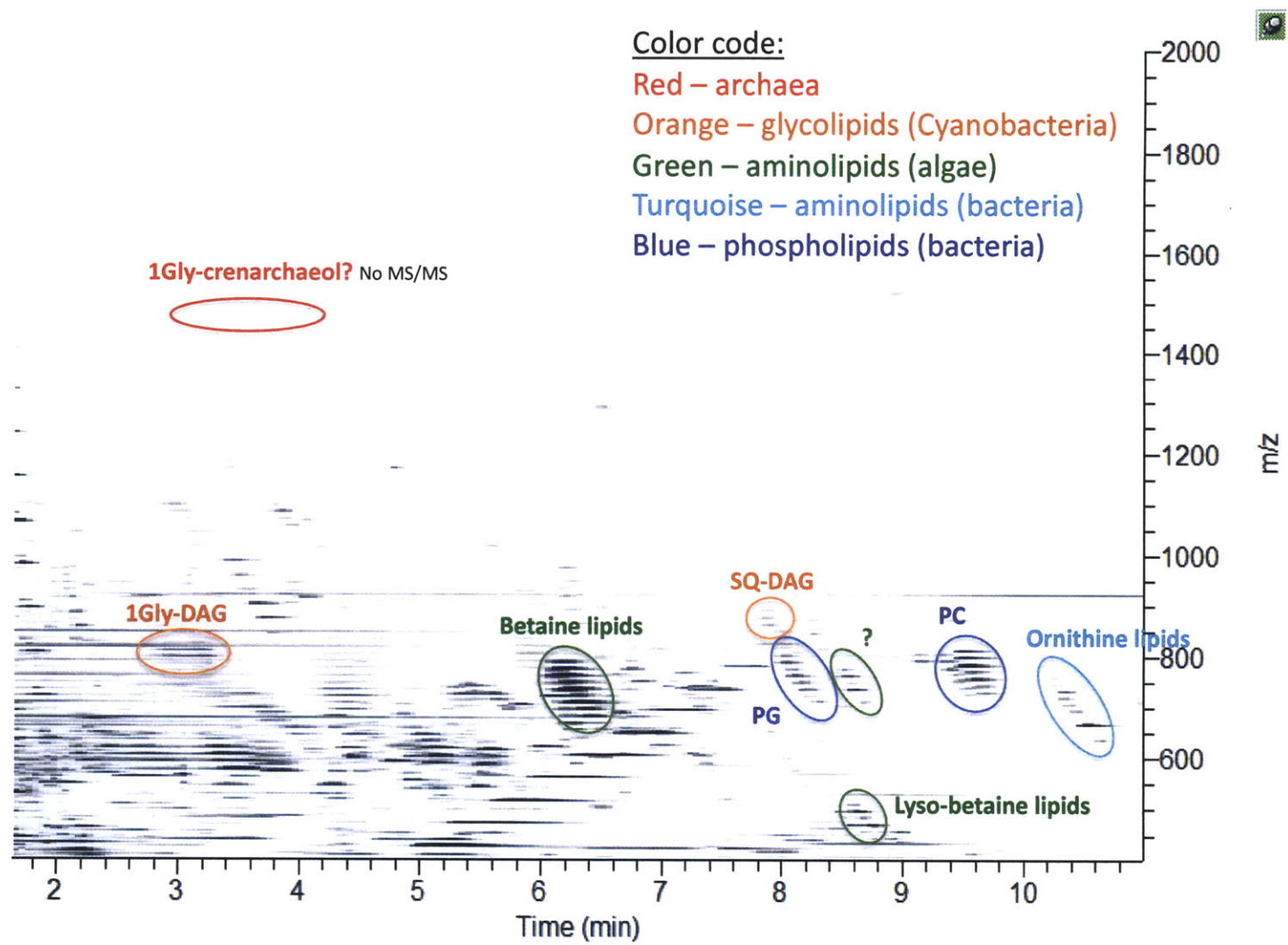
### ***Intact Polar Lipids (IPL) and Glycerol Dialkyl Glycerol Tetraethers (GDGTs)***

Using liquid chromatography we were about to identify larger lipid molecules (IPLs, GDGTs) that are inaccessible by traditional GC analysis. A number of molecules were identified that are attributed to archaeal and bacterial sources. Some of the IPLs found include monoglycosyl-diacylglycerol (1Gly-DAG) and SQ-diacylglycerol; here were also betaine lipids, ornithine lipids and phospholipids (See Figure 17).

Figure 18 depicts the chromatograms and structure of GDGTs of archaeal origin. The dominant molecule is crenarchaeol, which has five ring moieties; there are also significant amounts of GDGTs with 0, 1, 2, and 3 pentacyclic ring moieties (so-called GDGT-0, GDGT-1, GDGT-2, and GDGT-3). Figure 19 depicts the chromatograms and structures of GDGTs of bacterial origin, so-called branched GDGTs.



Figure 17: MS-MS data from Carpha ooid biofilm extract (d0), with the identities of major lipids listed.



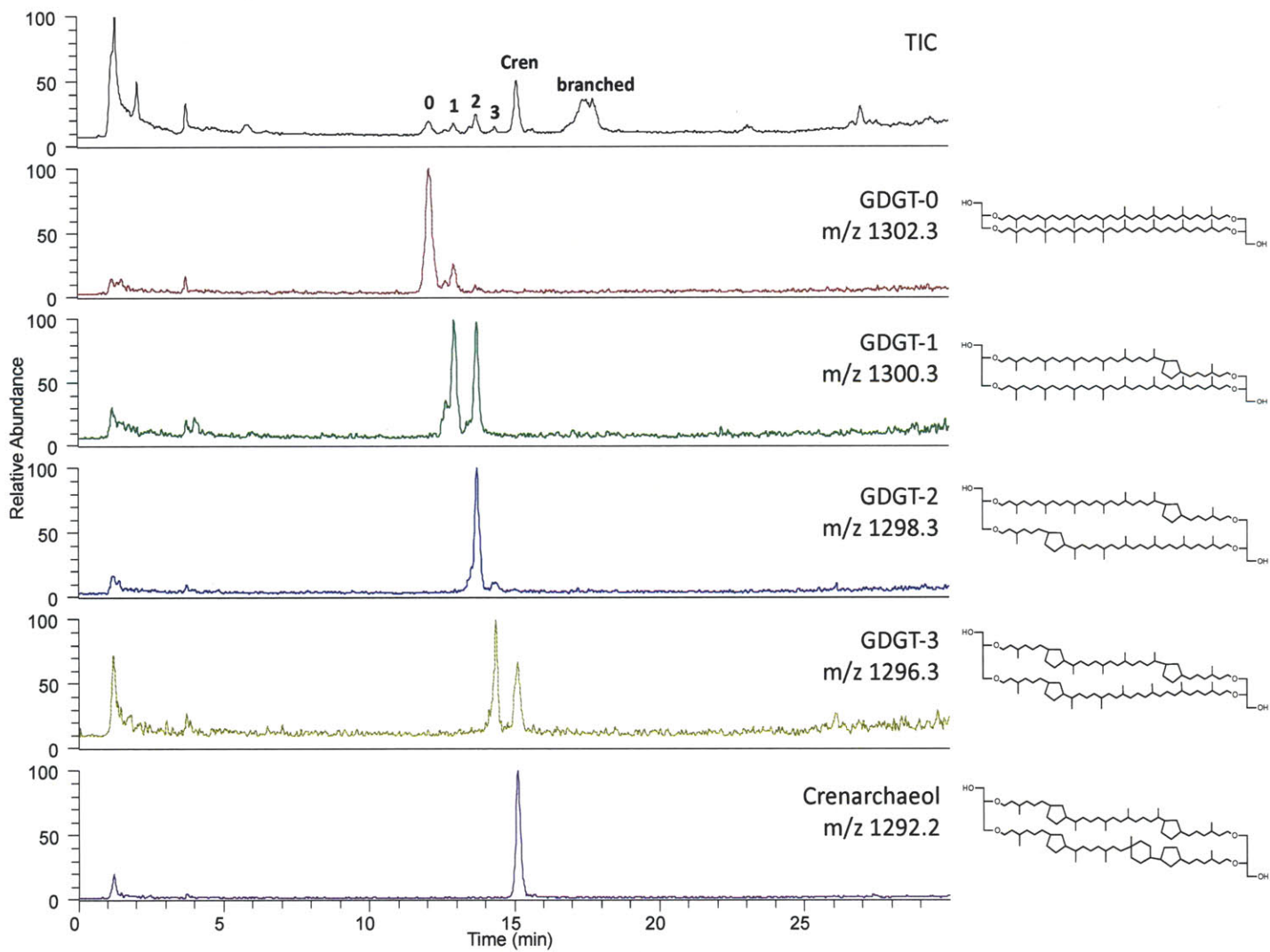
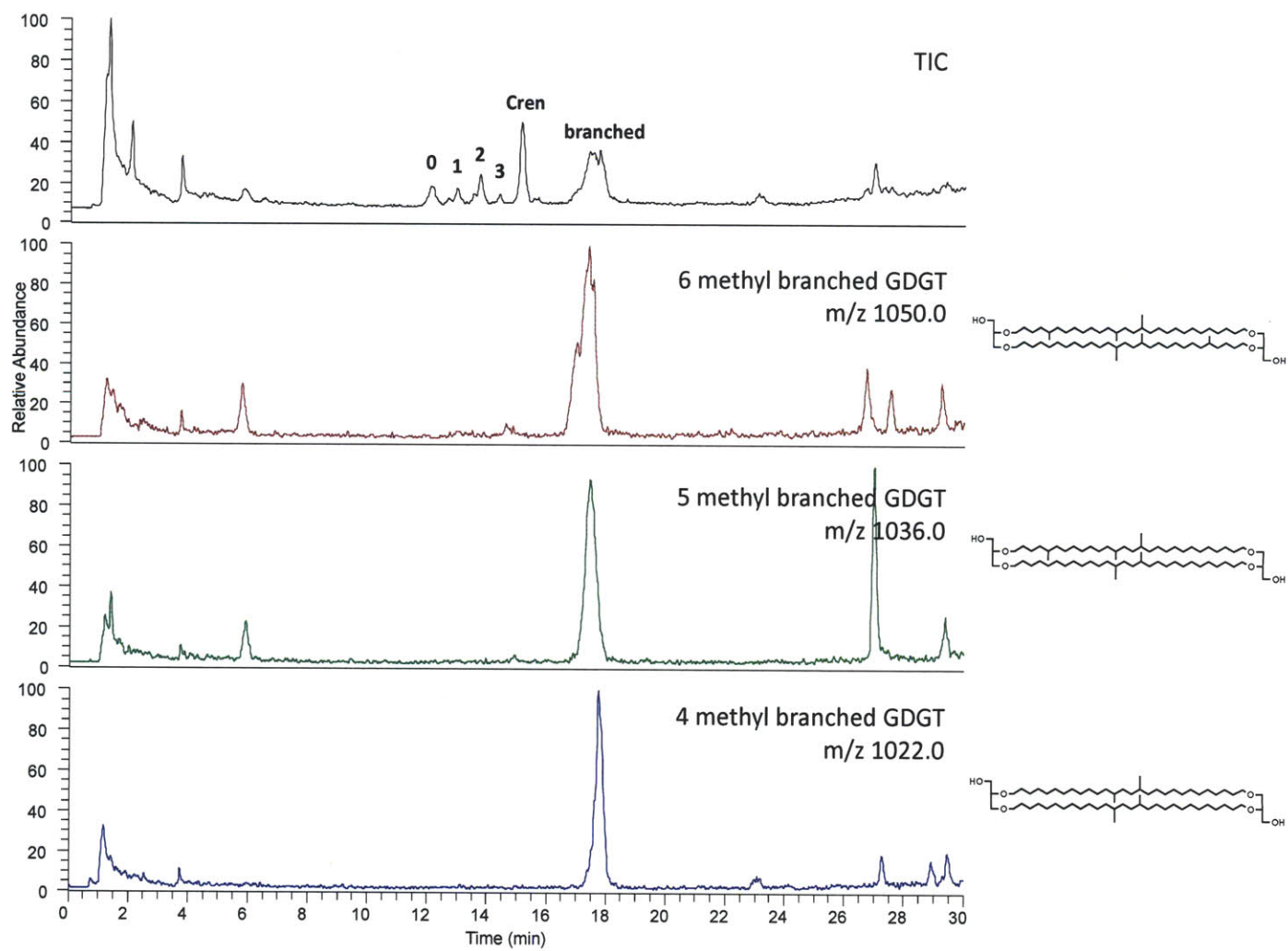


Figure 18: Chromatograms of GDGTs and the structure of archaeal GDGTs, extracted from *Carliia ooid* biofilm (d0).

Figure 19: Chromatograms of GDGTs and the structure of bacterial GDGTs, extracted from *Carbala ooid* biofilm (d0).



## Discussion

### *Elemental sulfur*

Reduced and/or elemental sulfur is a byproduct of the reduction of seawater sulfate by sulfate reducing bacteria (SRB). Although there was no sulfur in the biofilm of the Carbla ooids, we could smell sulfide when we collected the ooid samples from Hamelin pool, which suggests that sulfate reduction is occurring in the near-surface environment.

The fact that sulfur is incorporated into the ooid matrix throughout its growth suggests that the ooid has been growing in such an environment over its history. Perhaps the abundance of sulfur in the center of the ooid indicates that the geochemical environment created by sulfate-reduction is of particular importance during early ooid genesis.

### *Radiocarbon Dating of Organic Matter*

#### *Highborne Cay*

Because the small amount of material, even when clumped with adjacent extracts, was at the detection limit of the instrument, we believe that these values do not represent the actual age of the organic matter extracted from the ooids. These results informed our decisions for subsequent experiments (Carbla), mainly tripling the amount of raw material used and decreasing the number of dissolutions/extractions from 20 to 10, and led to what we believe is a better experiment with more representative data. It is difficult to interpret these data because there is no pattern, but perhaps the relatively old age of much of the extracted material suggests that much of the organic material was incorporated at the time of ooid formation, rather than new contributions from boring, colonizing bacteria. More work needs to be done on these samples in the future to get a better understanding of the age of the associated organic matter.

#### *Carbla*

Although the relationship is not perfect, there seems to be a general pattern of younger organic material in the first three measured samples (d0, d2, d4), and then older organic material in the later extracts (d6, d8). The data suggest that our hypothesis that the interior of the ooid contains organic material that is older, and that the organic matter “youngs” toward the surface of the ooid, especially when contrasted to the biofilm on the ooid’s exterior, but the relationship is not straightforward. One thing to remember when interpreting this data is that the dissolution experiment is likely not peeling back the entire sample of ooids, layer by layer, at once, although this was the goal. The signal the dissolutions record is likely to be averaged with neighboring extracts, so only the broadest trends are meaningful. Perhaps in future experiments, this can be improved.

## ***Radiocarbon Dating of Ooid Carbonate***

### *Highborne Cay*

These results suggest that ooid formation takes place over hundreds of years, and these particular ooids started forming at least 1000 years ago.

An interesting feature of the data that is present in all three ooid size fractions is a dip in  $^{14}\text{C}$  age when the ooid radius is approximately 70-80  $\mu\text{m}$ . This feature may have been borne out of an event that resulted in the erosion or dissolution of the outer laminations, such as a local or regional acidification event.

Another interesting feature of the data is that initial size of the ooid does not seem to matter much in the age of the ooid, just the current size. The smaller size fraction (.105 and .177 mm) is slightly younger than the originally larger (0.177 and .250 mm) fraction, once dissolved to the same size; but within error they appear to be roughly the same size. This could be the result of some proportion of the ooids dissolving, but it's unclear why only some of the ooids would be affected.

### *Carbla*

This data suggests that the surface of the ooid is ~200 years old, and that these ooids began forming at least 1250 years ago. If the observed trend continues to when the radius of the ooid is zero (minus some unknown nucleus dimension), they may have started forming over 2000 years ago.

Taken together, these sets of results indicate that modern ooid formation takes place over hundreds, and possibly thousands of years. The outer layer of these ooids is a few hundred years old. Although ooids may have laminae of varying sizes, suggesting discreet formation events, the age of the carbonate seems to step back smoothly as the ooid exterior is dissolved away, which could indicate a more gradual formation process than seems intuitive.

## ***Lipid distribution***

The FAMES in the Carbla ooid biofilm extract are dominated much more by the most common FAMES (n-C16,18) compared to the interior samples, which is not surprising due to their ubiquity in the environment. All of the extracts possess a similar overall pattern of FAMES including a suite of saturated, straight chain FAMES varying in length from C=14 to C=29 with a pronounced even-over-odd predominance. The even-over-odd pattern is a characteristic that is related to biosynthesis of fatty acids: carbons are added two at a time by a chain extended molecule onto a primer, so even numbered fatty acids are more common.

The sample also contain branched (iso, anteiso, and 10-methyl) short chain (C=14,15,16) FAMES. These are some of the most important biomarkers found in these samples because they occur commonly in sulfate reducing bacteria. Microbial reduction of sulfate can reduce the local concentration of sulfate and raise the alkalinity, which could have an effect on the precipitation of calcium carbonate to enhance ooid formation. Although sulfate reduction is ubiquitous in many environments and the ocean, it usually occurs in anaerobic environments, unlike the near surface, well mixed sample sites the ooids were collected from. Perhaps the ooids create microenvironments where sulfate reduction is favorable, which could further facilitate carbonate precipitation.

Many of the samples, including d0, the long (C=19-29) straight chain FAMES are preceded by a fatty ketone. The ketones did not exhibit the same pronounced even-over-odd pattern, so it is unclear if they are somehow related to their corresponding fatty acid, such as a degradation product. In terms of biological source or function, the ketones are enigmatic. They were too scarce in every sample to get hydrogen isotope data, which may help determine the biological source. In a future experiment in which more ooids are extracted, this may be possible.

The exterior lipids provides a snapshot of the microbial community that is living alongside the ooids today, and can be compared to other molecular techniques to more precisely understand the environment (Edgcomb et al., 2013); the lipids released upon dissolution, however, provide a more integrated picture of the microbial community over a longer period time. The consistent pattern seen throughout the dissolution suggests that the environment and microbial community remained fairly similar throughout the centuries of formation.

### ***Stable Carbon Isotopes***

The first order trend present in the straight chain saturated FAMES is lightest values in sample d0, increasing in samples d2 through d4, and then gradually decreasing again through sample d10. An interpretation of this pattern is that there has been consistent biological fractionation in lipid synthesis throughout ooid formation, but that the  $\delta^{13}\text{C}$  value of the starting material i.e. dissolved  $\text{CO}_2$  in the water, may have changed by a few ‰ over the duration of ooid formation.

One of the questions that arose during the project was the significance of the fatty ketones. We had hoped that isotopic evidence would help answer this question, but unfortunately it is still unclear, based on carbon isotope patterns, if the ketones derive from the same source as the long-chain FAMES.

## ***Hydrogen Isotopes***

### *Lipids*

Previous work has suggested that large  $\delta D$  variations in bacterial lipids are related to differences in metabolic pathways used by the synthesizing organism (Zhang et al., 2009). These results suggest that organisms with branched FAMES are utilizing a different metabolic pathway in the production of NADPH to create such drastic offsets from the majority of the fatty acids. This is one more indication of the complex microbial community that lives on and around ooids, and the lipids that are preserved within. This also supports the use of branched FAMES as biomarkers for organisms with metabolisms distinct from photoautotrophy i.e. sulfate reducing bacteria.

### ***Intact Polar Lipids (IPL) and Glycerol Dialkyl Glycerol Tetraethers (GDGTs)***

The identification of IPLs and GDGTs extracted from the Carbla ooid biofilm (d0) complement the analysis of FAMES by being more taxonomically specific polar-head groups than FAMES (although less geo-stable over long time periods). IPLs represent a portion of the living (or recently living) microbiota, while GDGTs are common archaeal membrane lipids. The IPL biomarkers point to a dominance of phototrophs: cyanobacteria (1Gly-DAG, SQ-DAG) and algae (betaine lipids). The sources of other identified IPLs (ornithine lipids and phospholipids) are bacterial, but not more specifically known.

The presence of both archaeal and bacterial GDGTs expands our understanding of the microbial community beyond just the bacterial domain. It is somewhat unusual that the archaeal derived lipids are dominated by crenarchaeol, which in other samples is more trace. We could further improve our understanding of this potentially unique archaeal community by molecular studies such as 16S-DNA.

## Conclusions

This work presents the first preliminary results of radiocarbon dating of ooid carbonate and organic carbon during sequential dissolution. Through analysis of the ooid carbonate we were able to determine that modern ooids form on a timescale of hundreds to a few thousand years. Specifically, Highborne Cay ooids began forming at least 1,000 years ago, with a possible erosional event approximately 500 years ago, and Carbla Beach ooids began forming at least 1,250 years ago. By analyzing the organic carbon liberated during dissolution, we gained insight into the process by which organics are preserved in ooids throughout their growth. Lipid analysis revealed biomarkers for a complex bacterial community, as previous research has demonstrated (Edgcomb et al., 2013; Summons et al., Under Review). Stable carbon and hydrogen isotopes allow us to further constrain the sources of some of the lipids. The source(s) of some of the compounds remains enigmatic.

Overall, this work supports the hypothesis of ooid cortex formation in two ways: first, that the presence of organic material facilitates ooid cortex formation, possibly protecting the forming ooid from dissolution and providing a scaffolding on which precipitation occurs; and second, that specific organisms, namely sulfate reducing bacteria, ameliorate carbonate precipitation in the local environment by altering the geochemistry in such a way as to make carbonate precipitation more favorable.

### ***Future Work***

A limitation of this project is the ability to determine the extent to which sequential dissolution and extraction of ooids is occurring radially, as intended. In the future, it will be useful to determine this by examining ooids microscopically throughout the dissolution process. As the experimental design for sequentially dissolving large amounts of ooids improves, we will continue to refine our understanding of ooid growth with respect to organic material and microbes.

If, as we and others have suggested, ooid formation and growth is partially dependent on and/or facilitated by a specific, complex microbial community, in addition to many other physical and chemical factors, it would be interesting and valuable to compare the microbial communities of nearby sediments in both ooid forming and non-forming regions. What are the differences in these communities, and what factors are controlling those differences? Another difference that would be interesting to investigate is that of marine and lacustrine ooid-forming sample sites. The unique geochemistry and microbial consortia of lacustrine environments could provide more insight into the conditions of ooid formation.



## Works Cited

- Allwood, A. C., M. R. Walter, B. S. Kamber, C. P. Marshall, and I. W. Burch, 2006, Stromatolite reef from the Early Archaean era of Australia: *Nature*, v. 441, p. 714-718.
- Brehm, U., W. E. Krumbein, and K. A. Palinska, 2006, Biomicrospheres generate ooids in the laboratory: *Geomicrobiology Journal*, v. 23, p. 545-550.
- Chave, K. E., 1965, Carbonates - Association with Organic Matter in Surface Seawater: *Science*, v. 148, p. 1723-&.
- Chave, K. E., and E. Suess, 1967, Suspended Minerals in Seawater: *Transactions of the New York Academy of Sciences*, v. 29, p. 991-&.
- Chave, K. E., and E. Suess, 1970, Calcium Carbonate Saturation in Seawater - Effects of Dissolved Organic Matter: *Limnology and Oceanography*, v. 15, p. 630-&.
- Davies, P. J., B. Bubela, and J. Ferguson, 1978, Formation of Ooids: *Sedimentology*, v. 25, p. 703-730.
- Decho, A. W., P. T. Visscher, and R. P. Reid, 2005, Production and cycling of natural microbial exopolymers (EPS) within a marine stromatolite: *Palaeogeography Palaeoclimatology Palaeoecology*, v. 219, p. 71-86.
- Duguid, S. M. A., T. K. Kyser, N. P. James, and E. C. Rankey, 2010, Microbes and Ooids: *Journal of Sedimentary Research*, v. 80, p. 236-251.
- Dupraz, C., and P. T. Visscher, 2005, Microbial lithification in marine stromatolites and hypersaline mats: *Trends in Microbiology*, v. 13, p. 429-438.
- Edgcomb, V. P., J. M. Bernhard, D. Beaudoin, S. Pruss, P. V. Welander, F. Schubotz, S. Mehay, A. L. Gillespie, and R. E. Summons, 2013, Molecular indicators of microbial diversity in oolitic sands of Highborne Cay, Bahamas: *Geobiology*, v. 11.
- Liu, X., J. S. Lipp, and K.-U. Hinrichs, 2011, Distribution of intact and core GDGTs in marine sediments: *Organic Geochemistry*, v. 42, p. 368-375.
- Liu, X. L., R. E. Summons, and K. U. Hinrichs, 2012, Extending the known range of glycerol ether lipids in the environment: structural assignments based on tandem mass spectral fragmentation patterns: *Rapid Communications in Mass Spectrometry*, v. 26, p. 2295-2302.
- Mitterer, R. M., 1968, Amino Acid Composition of Organic Matrix in Calcareous Oolites: *Science*, v. 162, p. 1498-&.
- Mitterer, R. M., 1972, Biogeochemistry of Aragonite Mud and Oolites: *Geochimica Et Cosmochimica Acta*, v. 36, p. 1407-&.
- Noffke, N., D. R. Christian, and R. M. Hazen, 2011, A (Cyano-)Bacterial Ecosystem in the Archaean 3.49 Ga Dress Formation, Pilbara, Western Australia, GSA Annual Meeting, Minneapolis, MN.
- Osburn, M. R., A. L. Sessions, C. Pepe-Ranne, and J. R. Spear, 2011, Hydrogen-isotopic variability in fatty acids from Yellowstone National Park hot spring microbial communities: *Geochimica Et Cosmochimica Acta*, v. 75, p. 4830-4845.
- Paul, J., T. M. Peryt, and R. V. Burne, 2011, Kalkowsky's Stromatolites and Oolites (Lower Buntsandstein, Northern Germany), *Advances in Stromatolite Geobiology: Lecture Notes in Earth Sciences*, Springer Berlin Heidelberg, p. 13-28.

- Plee, K., D. Ariztegui, R. Martini, and E. Davaud, 2008, Unravelling the microbial role in ooid formation - results of an in situ experiment in modern freshwater Lake Geneva in Switzerland: *Geobiology*, v. 6, p. 341-350.
- Reitner, J., G. Arp, V. Thiel, P. Gautret, U. Galling, and W. Michaelis, 1997, Organic matter in Great Salt Lake ooids (Utah, USA) - First approach to a formation via organic matrices: *Facies*, v. 36, p. 210-219.
- Sandberg, P. A., 1975, New Interpretations of Great Salt Lake Ooids and of Ancient Non-Skeletal Carbonate Mineralogy: *Sedimentology*, v. 22, p. 497-537.
- Simone, L., 1981, Ooids - A Review: *Earth-Science Reviews*, v. 16, p. 319-355.
- Summons, R. E., L. R. Bird, A. L. Gillespie, S. B. Pruss, M. Roberts, and A. L. Sessions, Under Review, Lipid biomarkers in ooids from different locations and ages: evidence for a common bacterial flora: *Geobiology*.
- Wang, Y., and A. L. Sessions, 2008, Memory Effects in Compound-Specific D/H Analysis by Gas Chromatography/Pyrolysis/Isotope-Ratio Mass Spectrometry: *Analytical Chemistry*, v. 80, p. 9162-9170.
- Zhang, X., A. L. Gillespie, and A. L. Sessions, 2009, Large D/H variations in bacterial lipids reflect central metabolic pathways: *Proceedings of the National Academy of Sciences of the United States of America*, v. 106, p. 12580-12586.